Validation and parametrization of the soil moisture index for stomatal conductance modelling and flux-based ozone risk assessment of

Citation for the original published paper (version of record):
Carrasco-Molina, T., Marzuoli, R., Calatayud, V. et al (2024). Validation and parametrization of the soil moisture index for stomatal conductance modelling
and flux-based ozone risk assessment of Mediterranean plant species. Agricultural and Forest Meteorology, 354. http://dx.doi.org/10.1016/j.agrformet.2024.110080

(article starts on next page)

Agricultural and Forest Meteorology 354 (2024) 110080

Contents lists available at ScienceDirect

Agricultural and Forest Meteorology

journal homepage: www.elsevier.com/locate/agrformet

Validation and parametrization of the soil moisture index for stomatal conductance modelling and flux-based ozone risk assessment of Mediterranean plant species

Tania Carrasco-Molina [a,b,*], Riccardo Marzuoli [c], Vicent Calatayud [d], David Simpson [e,f], Giacomo Gerosa [c], Arnaud Carrara [d], Isaura Rábago [a], Rocío Alonso [a], Ignacio González-Fernández [a]

[a] Ecotoxicology of Air Pollution, CIEMAT, Madrid, Spain
[b] Dept. of Biology, Geology, Physics and Inorganic Chemistry. Escuela Internacional de Doctorado, Universidad Rey Juan Carlos, Móstoles, Madrid, Spain
[c] Dept. of Mathematics and Physics, Catholic University of the Sacred Heart, Brescia, Italy
[d] Fundación CEAM, Paterna, Valencia, Spain
[e] EMEP MSC-W, Norwegian Meteorological Institute, Oslo, Norway
[f] Dept. Space, Earth & Environ. Chalmers University of Technology, Gothenburg, Sweden

ARTICLE INFO

Keywords:
Phytotoxic ozone dose (POD)
Leaf water potential
Drought
Quercus ilex
Broadleaf deciduous Mediterranean oaks
Mediterranean annual pastures

ABSTRACT

The Mediterranean region chronically experiences high levels of tropospheric ozone (O_3) that can affect the health of vegetation. However, limiting plant growing conditions, such as low soil moisture, may restrict the stomatal phytotoxic ozone dose (POD) absorbed by vegetation, modulating O_3 detrimental effects. Atmospheric chemistry transport models that estimate POD for O_3 risk assessment of effects on vegetation species, such as the European Monitoring and Evaluation Programme (EMEP), have adopted the soil moisture index (SMI) to consider the influence of soil moisture on POD. The objectives of this study were the parametrization and validation of the SMI effect on stomatal conductance (g_s) for improving the POD estimation and O_3 risk assessment for different vegetation species under water-limiting growing conditions, using field data collected in Italy and Spain and a literature review. The modelled SMI from EMEP proved to be a good indicator of soil moisture dynamics across sites and years, although it showed a general tendency to overestimate soil moisture availability for plants, particularly in the driest seasons. New parametrizations derived for modelling SMI effects on g_s under Mediterranean conditions proposed in this study stress the importance of using species-specific parameters for species showing contrasting water-saving strategies in contrast of the current approach of using a simple relation between SMI and g_s for all the species. Furthermore, g_s modelling parametrizations based on soil water potential (SWP) were found to be more suitable than SMI for local scale estimation of POD under water-limiting conditions. Further consideration of rooting depth and distribution will be required in the future to determine the soil depth at which the soil moisture should be measured in POD modelling, since these features represent one of the most important uncertainties affecting the estimation of POD that could not be addressed with the present database.

1. Introduction

The Mediterranean Basin is generally considered at risk due to the effects of air pollution (Fuhrer et al., 2016; Ochoa-Hueso et al., 2017). Tropospheric ozone (O_3) levels, an oxidizing secondary air pollutant, are chronically high in this region due to the anticyclonic conditions, intense solar radiation, and elevated temperatures common to the Mediterranean climate, that favor the photochemical reactions that produce O_3 (Kalabokas et al., 2007; Zanis et al., 2014; Fuhrer et al., 2016; Ochoa-Hueso et al., 2017; European Environment Agency, 2023). Consequently, the Mediterranean region experiences elevated surface O_3 levels (Mills et al., 2018; Dafka et al., 2021), exceeding recommended levels for preserving vegetation health (Guerreiro et al., 2018; Jakovljević et al., 2021).

* Corresponding author at: Ecotoxicology of Air Pollution, CIEMAT (Edif.70). Avda. Complutense nº40, Madrid 28040, Spain.
E-mail address: Tania.Carrasco@ciemat.es (T. Carrasco-Molina).

https://doi.org/10.1016/j.agrformet.2024.110080
Received 22 December 2023; Received in revised form 9 April 2024; Accepted 20 May 2024
Available online 4 June 2024

The effects of O_3 on Mediterranean vegetation have been widely studied. Studies have reported negative effects of O_3 on Mediterranean European ecosystems under experimental and field conditions, including foliar injury, tree crown defoliation, biomass growth decrease and effects on reproductive ability, forage quality and plant community structure and composition (Calatayud et al., 2011; Mills et al., 2011; Calvete-Sogo et al., 2014; Alonso et al., 2014; Sanz et al., 2015; Sicard et al., 2016; Diaz-de-Quijano et al., 2016; Marzuoli et al., 2018; Fuhrer et al., 2016; Jakovljević et al., 2021; Agathokleous et al., 2020).

Ozone effects are better related with the stomatal absorbed dose, or phytotoxic O_3 dose above a threshold of "y" nmol m^{-2} s^{-1} (POD_y), than with the concentration of this pollutant in the atmosphere (Mills et al., 2011; CLRTAP, 2017; Emberson, 2020). Ozone is absorbed through the stomata during the normal gas exchange and induces the production of reactive oxygen species affecting plant metabolism (Wohlgemuth et al., 2002; Grulke and Heath, 2020; Juráň et al., 2021), although part of them can be quenched through detoxification and repair mechanisms (Castagna and Ranieri, 2009; Pellegrini et al., 2019). POD_y varies between species depending on plant traits and environmental growing conditions, which influence stomatal aperture, and thus the O_3 exposure.

In agreement with this, O_3 risk assessment methodologies employed by the Convention on Long-range Transboundary Air Pollution (CLRTAP) are based on POD_y estimates (CLRTAP, 2017). The POD_y is calculated, following the CLRTAP methodology, using species-specific parametrizations of a stomatal conductance (g_s) model, which was defined through a Jarvis multiplicative approach (Jarvis, 1976; Emberson et al., 2000; CLRTAP, 2017). These parametrizations describe how environmental growing conditions such as air temperature and relative humidity, solar radiation or soil moisture availability limit the stomatal aperture and the amount of O_3 absorbed by plants.

Despite the high O_3 concentrations during spring and summer, POD_y values for Mediterranean vegetation species are generally restricted by strong limitations caused by environmental factors, of which the soil moisture availability is one of the most important (Simpson et al., 2003; Anav et al., 2018; Guaita et al., 2023). Many Mediterranean ecosystems are located in water-limited areas (Nardini et al., 2014), and water stress is expected to spread under future climate change (Naumann et al., 2018). Soil moisture also varies seasonally, along with temperature and rainfall, affecting plant metabolism and promoting adaptations to the growing conditions (Viola et al., 2008; Keenan et al., 2009). Vegetation species from this region present different water use and saving strategies (Viola et al., 2008; Quero et al., 2011) that can modify species responses to drought. The distribution of the root system, the hydraulic architecture or the stomatal control are some of the factors that can differentiate plant water potential dynamics among species in response to limiting soil moisture availability (Martínez-Vilalta and Garcia-Forner, 2017).

Considering the important influence of soil moisture under current, as well as future, climatic conditions, it appears of particular importance to represent adequately the influence of soil moisture on g_s and POD_y for O_3 risk assessment. Different schemes have been proposed to model the g_s response to soil drying (Verhoef and Egea, 2014; Büker et al., 2012; Simpson et al., 2012) based on different soil moisture metrics. The methodology for calculating POD_y adopted by the CLRTAP for O_3 risk assessment considers the simplest scheme (*sensu* Verhoef and Egea, 2014), where the soil moisture, expressed as soil water potential (SWP), soil water content (SWC) or plant available water (PAW), at a certain depth, directly limits the g_s as described by a species-specific response function (CLRTAP, 2017). The European Monitoring and Evaluation Programme's Meteorological Synthesizing Centre West (EMEP MSC-W) chemical transport model (Simpson et al., 2012, 2022) uses the soil moisture index (SMI), a product from the European Centre for Medium-Range Weather Forecasts (ECMWF) Integrated Forecasting system (IFS) hydrological model (Balsamo et al., 2009; ECMWF, 2021a, 2021b), with a simple function between SMI and g_s for all vegetation types at a certain depth (termed as default or general parametrization). The SMI (ranging between 0 and 1) is an indicator of soil moisture computed by normalizing the SWC between the wilting point and the field capacity (SMI=1).

In this context, the present study aims at improving the estimation of g_s and POD_y under water-limited growing conditions in the Mediterranean area by: (i) comparing modelled and observed SMI data at three field sites in Italy and Spain; (ii) parameterizing the response of g_s to SMI and SWP for Mediterranean vegetation species used in O_3 risk assessment, testing whether different measurement conditions affect the parametrization result, based on field and literature derived g_s data; and (iii) evaluating how the different factors and parametrizations affect POD_y estimation at the plot scale using monitoring data collected at three field sites in Italy and Spain.

2. Material and methods

2.1. Field monitoring sites and SMI modelled values

Three field monitoring sites with continuous records of O_3 concentration, meteorology and soil moisture were considered to validate the use of modelled SMI values and the implications for POD_y estimation at the plot scale within the 2010–2015 timeframe. The monitoring sites were located in central and western Spain (Tres Cantos, TC, and Majadas del Tiétar, MJD), and in the Po Plain of northern Italy (Bosco Fontana, BF), as illustrated by the stars in Fig. 1.

Table 1 describes the location, characteristics and measurements included in this study for each monitoring site as well as the time period considered in each case depending on the information available. A more detailed description of each site is available in García-Gómez et al. (2016a, 2016b) (TC), El-Madany et al., 2018 (MJD) and Gerosa et al., 2022 (BF).

Hourly O_3 concentrations needed for POD_y estimation were monitored on-site in BF and at 1 km from the soil moisture and meteorology monitoring plot in TC. O_3 concentrations in MJD were taken from a monitoring station located in Monfragüe, 17 km from the study site under comparable conditions in terms of landscape and influence of atmospheric pollution sources. A comparison of more recent O_3 concentrations recorded on-site in MJD with the monitoring station in Monfragüe shows a very close correlation. Ozone concentrations measured at reference height were corrected to canopy height (8 m for broadleaf evergreen forest species and 0.2 m semi-natural annual pastures) using a tabulated gradient (CLRTAP, 2017; values were derived from earlier EMEP model runs for a summer period) in MJD and TC. Full atmospheric correction of O_3 concentrations at canopy height in TC and MJD was not possible due to insufficient information at the O_3 monitoring sites; however, the tabulated gradients correction is considered a simple, good method for forest ecosystems (Gerosa et al., 2017). No correction was performed in BF since O_3 concentrations were already measured at the canopy height (26 m above ground on a micrometeorological tower).

Continuous records of SWC at different depths of each monitoring site were used to calculate observed SMI values following Simpson et al. (2012) as outlined in Eq. (1):

$$SMI = (SWC - SWC_{min})/(SWC_{max} - SWC_{min}) \quad (1)$$

Where SWC_{max} and SWC_{min} are the maximum and minimum SWC, which are alternatively referred as field capacity (FC) and wilting point (WP). FC and WP values were obtained for each site using the van Genuchten (VG) model (van Genuchten, 1980), with model parameters estimated using the pedotransfer functions (Szabó et al., 2021) based on soil characteristics measured at the study sites in BF and MJD. In TC, soil hydraulic parameters were obtained by fitting the VG model to soil water retention curves obtained in the laboratory from undisturbed soil samples collected at the depth of the sensor in the vicinity of the measurement point. The WP was calculated with the VG model using a species-specific water potential according to the data reported in the

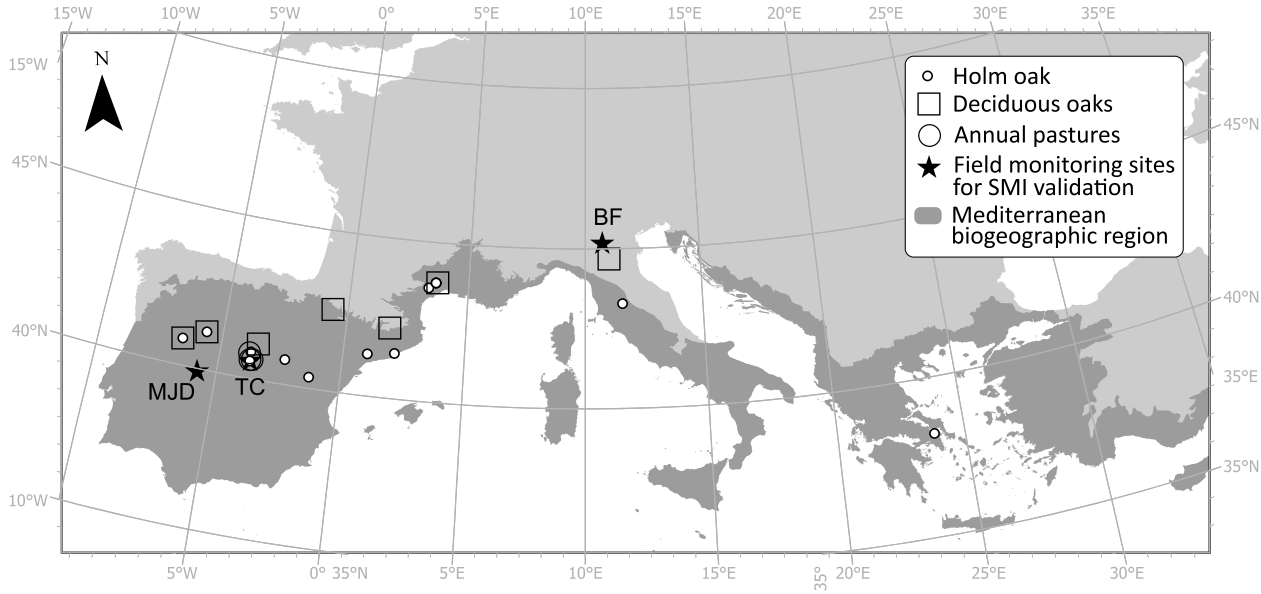

Fig. 1. Location of the sites used for the parametrization of holm oak (little dots), deciduous oaks (squares) and annual pastures functional types (big dots). Location of the monitoring sites used for SMI validation, Majadas del Tiétar (MJD), Tres Cantos (TC) and Bosco Fontana (BF) are also represented with black stars.

literature reviewed (Tables A1 and A2 from the Appendix A of the Supplementary material).

In the EMEP model, SMI is used to indicate soil water stress, as it is measure of PAW that is very suitable for interpolating across the heterogeneous vegetation and soil types (Gao et al., 2016; Hunt et al. 2009). In the IFS model (ECMWF, 2021a, 2021b), SMI is calculated for different sub-grid vegetation/soil patches. Then, these values are spatially interpolated to the 0.1 × 0.1° longitude/latitude resolution used by EMEP. SMI modelled values for the field sites were extracted from the nearest 0.1° grid cell. The IFS model uses a revised hydrological module in the Tiled ECMWF Scheme for Surface Exchanges over Land (H-TESSEL) to obtain soil moisture at different soil layers, in which the spatial variation of soil texture is considered to produce SMI values. This scheme estimates the FC and WP at fixed matric potentials of −0.01 and −1.5 MPa, respectively, depending on soil texture (Balsamo et al., 2009; ECMWF, 2021a, 2021b). Following the methodology for POD_y estimation of the EMEP model described by Simpson et al. (2012), the modelled SMI representative of the soil layer depth between 28 and 100 cm (termed as SMI3), was compared with the observed SMI values.

2.2. Literature and field data on g_s response to soil moisture

The scientific literature was reviewed to collate a database on g_s response to soil moisture for *Quercus ilex* (Aguadé et al., 2015; Alonso et al., 2008; Castell et al., 1994; Filho et al., 1998; Forner et al., 2018; Limousin et al., 2009; Mediavilla and Escudero, 2003; Misson et al., 2010; Pardos et al., 2005; Rambal et al., 2003; Rhizopoulou and Mitrakos, 1990; Tognetti et al., 1998), as representative species of broadleaf evergreen Mediterranean forest species, and *Q. faginea, Q. pyrenaica, Q. pubescens, Q. petraea* and *Q. robur* (Aranda et al., 2000; Damesin and Rambal, 1995; Grassi and Magnani, 2005; Martín-Gómez et al., 2017; Mediavilla and Escudero, 2003; Poyatos et al., 2008), as representative of deciduous oak species. The review included all field studies in the Mediterranean biogeographic region of Europe reporting g_s and soil moisture data, either as pre-dawn leaf water potential (LWP), SWP or SWC, together with site coordinates or site-specific soil characteristics.

Fig. 1 presents the location of the studies considered to build the g_s response to soil moisture database. Other details of the studies included in the literature review are provided in the Table A1, where a total of 17 studies from 4 countries (Italy, France, Greece and Spain) were considered. The g_s data included observations at leaf, branch or canopy scales measured using infrared gas analyzer, porometer, sapflow and eddy covariance techniques. Out of the 12 studies reviewed on *Q.ilex*, 3 were conducted in clay loam soils, 3 in silty clay loam soils and 1 in sandy soils, with contrasting soil depths. Regarding g_s measurement techniques, 1 of them used eddy covariance, 9 IRGA or porometer portable gas exchange system at the leaf level and 2 sapflow. For deciduous oaks 6 studies have been reviewed (also Pardo et al., 1997 to consult the soil characteristics of Aranda et al., 2000), in which infrared gas analyzer was uniformly used as a technique to measure g_s.

A database on g_s response to soil moisture for annual Mediterranean pasture species was built from field measurements collected during 5 independent sampling campaigns (2005, 2007, 2010, 2011 and 2012) from three sites (Miraflores, TC and Viñuelas) in central Iberian Peninsula. Some data were already published by Alonso et al. (2007a) and González-Fernández et al. (2010) while new g_s data from TC was specifically considered in this study. The g_s of legume, grass and forb species was measured at the leaf level with a LICOR-6400 infrared gas analysis system (LiCor Inc., Lincoln, NE, USA) at all sites. Soil moisture was measured with a Time-domain Reflectometer at 15 cm in Miraflores and Viñuelas (TRIMEGM, IMKOGmbH, Germany) and with an Enviroscan sensor (Sentech Technologies, Australia) at 20 cm depth in TC. More details of the field sites where annual pastures were measured are provided in Supplementary Material (Table A1).

All soil moisture observations included in the g_s response to soil moisture database were transformed to either SWP and/or SMI. The predawn LWP has been assumed to be equivalent to the SWP (Richter, 1997; Levin and Nackley, 2021). SWP was transformed to SMI using the VG model (van Genuchten, 1980). Soil hydraulic properties were obtained from site-specific soil information, from pedotransfer functions (Szabó et al., 2021) using soil data measured at the study sites, or from the European Soil Hydraulic Database (Tóth et al., 2017) extracting data at site coordinates. The latter source was used at a resolution of 1 km and at a depth of 60 cm, for consistency with most soil monitoring sensor depths and SMI3 modelled values. Pedotransfer functions and soil hydraulic property map variables were extracted using R packages raster and euptf2 (Hijmans, 2023; Weber et al., 2020).

2.3. Parametrization of soil moisture functions for g_s.POD_y calculation and sensitivity analysis

POD_y was calculated at the plot scale for the three sites (BF, MJD and

Table 1
Field monitoring sites considered in this study for SMI validation and POD_1 estimation at the plot scale. Temperature, rainfall and ozone are presented for the period considered in each case. Ozone concentration is expressed as the mean of the 12-hour growing season.

	Tres Cantos (TC, Spain)	Bosco Fontana (BF, Italy)	Majadas del Tiétar (MJD, Spain)
Coordinates	40°35′16.80″N,3°43′58.80″W	45°12′02″N,10°44′44″E	39°56′29″N,5°46′24″W
Period considered	2010–2015	2013–2015	2011–2015
Type of vegetation	Broadleaf evergreen forest, abandoned dehesa of *Quercus ilex*	Broadleaf deciduous forest of *Quercus robur* and *Carpinus betulus*	Broadleaf evergreen forest, open dehesa of *Quercus ilex*
Soil texture	Sandy loam (0–100 cm), sandy clay loam (100–200 cm)	Loam/sandy loam	Sandy loam
Soil moisture sensor depth (cm)	20, 50 and 100	30	8 and 40
Type of soil moisture sensor	Capacitance	Time domain reflectometry	Capacitance
Mean annual temperature (°C)	14.6	13.5	16.7
Mean annual rainfall (mm)	337.5	985	550
Ozone concentration (ppb)	40.3	49.7	39.1

TC) in Table 1, following the methodology described in Chapter III of the Modelling and Mapping Manual (CLRTAP, 2017). This methodology is based on the Deposition of O_3 and Stomatal Exchange (DO_3SE) model (Emberson et al., 2000, 2001), which uses a multiplicative algorithm (Jarvis, 1976) for estimating g_s values that are needed for POD_y calculation, following Eq. (2):

$$g_s = g_{max} * f_{phen} * f_{light} * max\left\{g_{min}, \left(f_{temp} * f_{VPD} * f_{SWP}\right)\right\} \quad (2)$$

Where g_{max} is a species-specific maximum g_s value and g_{min} is the minimum conductance during the daylight time.f_{phen}, f_{light}, f_{temp}, f_{VPD} and f_{SWP} are modifying functions, scaled from 0 to 1, that describe how plant phenology and environmental factors, including photosynthetic active radiation, temperature, vapour pressure deficit and soil moisture, affect stomatal aperture, respectively. Adequate g_s modelling parametrizations described in the Modelling and Mapping Manual (CLRTAP, 2017) were considered for POD_y estimation at each of the three field sites according to the vegetation in the area: deciduous oak forest species in BF, and broadleaf evergreen forest species and Mediterranean annual legume species in MJD and TC (CLRTAP, 2017). Appendix B presents further details on the methodology for POD_y estimation and the Mapping Manual parametrizations employed. Following the parametrization for these vegetation types, the POD_y flux threshold selected for detoxification was 1 nmol m^{-2} s^{-1}.

The g_s limiting functions due to soil moisture (expressed as SMI or SWP – f_{SMI} or f_{SWP}, respectively) were fitted with boundary line analysis as described below. In contrast to the f_{SWP} parametrization from the Mapping Manual (CLRTAP, 2017), an exponential function has been fitted to describe the response of g_s to SWP as indicated by the data from the literature reviewed. For *Q.ilex*, the species with the largest database, regression analyses were conducted to characterize the influence of g_s measurement technique (IRGA/porometer at the leaf level, eddy covariance, sap flow), soil texture (clay loam and silty clay loam) and soil depth (deep or shallow corresponding to greater or smaller than 50 cm soil depth) on f_{SMI} and f_{SWP} parametrizations. Regression analyses were also conducted to test for differences in soil moisture functions between functional types of Mediterranean annual pastures.

The ability of newly developed soil moisture limiting functions (SMI and SWP) for g_s modelling was tested against g_s measured under field conditions. Published g_s data from two sites in central Spain were used for *Q. ilex* (n = 208) and compared with modelled g_s data obtained using the local parametrizations of f_{phen}, fl_{ight}, f_{temp} and f_{VPD} (Alonso et al., 2007b, 2008). For annual pastures, field data measured on *Trifolium* species from 3 sites in central Spain was considered (n = 54, Table A1). The new soil moisture limiting functions were also compared with the general SMI function for all the species in the case of *Q.ilex* and with the available f_{SWC} for annual pastures (González-Fernández et al., 2010).

The soil moisture limiting effect on POD_1 at each site was estimated considering two soil moisture functions, based on SMI (f_{SMI}) and SWP (f_{SWP}), in the calculation of g_s following Eq. (2). For SMI, a sensitivity analysis was conducted to estimate the consequences for POD_1 estimation for different vegetation types due to differences in soil moisture data source (observed or modelled SMI data), soil moisture monitoring depth (<28, 28–100 or ≥100 cm depth) and soil moisture parametrization (standard versus species-specific parametrization). The effect of changing soil depth was conducted different depending on the species. For annual pastures POD_1 values were obtained employing soil moisture records at <28 cm depth at each site (8 cm at MJD and 20 cm at TC) and compared with POD_1 estimates from soil moisture observations at <100 cm (40 and 50 cm in MJD and TC, respectively). For holm oak, POD_1 was calculated with soil moisture records at 100 cm depth, compared with soil moisture at 50 cm depth. The standard parametrization refers to the default f_{SMI}, with a SMI threshold of 0.5 (referred to in this study as critical SMI, SMI_{crit}) indicating the start of soil

moisture limitation for g_s (Simpson et al., 2012). Differences between the existing f_{SWC} and the new f_{SWP} for annual pastures were also studied. For forest tree species, the effect of using the existing Modelling and Mapping Manual (CLRTAP, 2017) f_{SWP} versus the new exponential shaped f_{SWP} developed in this study was compared.

Following the growing season of the predominant vegetation of each site as well as the available data, POD_1 was calculated at TC and MJD from 2011 to 2015 and at BF from 2013 to 2015. At the Spanish sites, POD_1 was estimated per hydrological year, from 1st October to 30th September of the following year, for both *Q.ilex* (termed as MJD_MEDevg and TC_MEDevg, respectively) and annual pastures (termed as MJD_MEDap and TC_MEDap, respectively). In BF, the POD_1 was calculated between 1st April and 30th September per calendar year for deciduous oaks (termed as BF_MEDdo).

Since differences in POD_1 among sites can arise from different reasons, such as O_3 correction to canopy height protocols, g_s parametrizations or site-specific growing conditions when comparing results within sites, all POD_1 values were expressed as percentages relative to POD_1 estimated using observed soil moisture at soil depths ≥28 cm and <100 cm depth, coincident with the SMI3 soil layer, and a species-specific soil moisture function applied at each site.

2.4. Statistical analyses

Modelled SMI3 and observed SMI values at different depths in the field sites were compared following the methodology described in Albergel et al. (2012a). Taylor diagrams (Taylor, 2001) were produced with the openair and plotrix packages (Carslaw and Ropkins, 2012; Lemon, 2006) in R, comparing modelling results across sites and different temporal scales (all dataset, years, seasons and months). Each point in the diagrams reflects a comparison between an observed and modelled value. The angle at which each point is located represents the degree of correlation (R) between the observed and modelled data, while the distance between each point and the point on the x-axis representing the observed value reflects the normalized standard deviation (SDV). These statistics are related by the centered normalized root mean square difference $\left(E = \sqrt{SDV^2 + 1 - 2{*}SDV{*}R}\right)$, shown by the distance between each point and the observed value on the x-axis (Taylor, 2001; Albergel et al., 2012a). Low values of E indicate higher similarity between observed and modelled values.

The g_s limiting functions due to soil moisture, f_{SWP} and f_{SMI}, were fitted with boundary line analysis (Chambers et al., 1985; Schmidt et al., 2000), based on relative g_s data per study site, using Eqs. (3) and (4). Maximum g_s was found by averaging g_s values above the 95th percentile for each site and species. The points that determine the boundary line were calculated by subsetting the SMI or water potential range, for which the 99th percentile of the relative g_s associated with these intervals was calculated. The f_{SWP} boundary line was fitted using nonlinear regression (Eq. (3)) via the nls function from stats package (R Core Team, 2022) in R, by setting the maximum conductance as 1. The point in f_{SWP} at which the relative g_s has a value of 1 and from which it begins to decrease is known as maximum SWP (SWP_{max}). Minimum SWP (SWP_{min}) was estimated for forest tree species when f_{SWP} reached a stable relative g_s value. The stable g_s value was estimated as the average relative g_s below the minimum LWP values established in Table A2 for each species. For annual pastures, SWP_{min} was established when g_s reached a minimum value of 0.02, following the existing f_{min} parametrization for annual pasture species (CLRTAP, 2017). The f_{SMI} was determined using a linear regression (Eq. (4)) with the lm function from stats package in R (R Core Team, 2022). The maximum relative g_s value is limited to 1, which gives the value of SMI_{crit}.

$$relative\ g_s = \min(1; a * \exp(b * SWP)) \tag{3}$$

$$relative\ g_s = \min(1; a + b * SMI) \tag{4}$$

The goodness of fit of g_s models considering different soil moisture functions and parametrizations was evaluated by linear regression against g_s field measurements from Alonso et al. (2008) for holm oak and all field data for annual pasture species (Table A1). The g_s models were compared based on linear regression slope, R^2 and root mean square error (RMSE).

Regression analyses were performed with car and stats packages (R

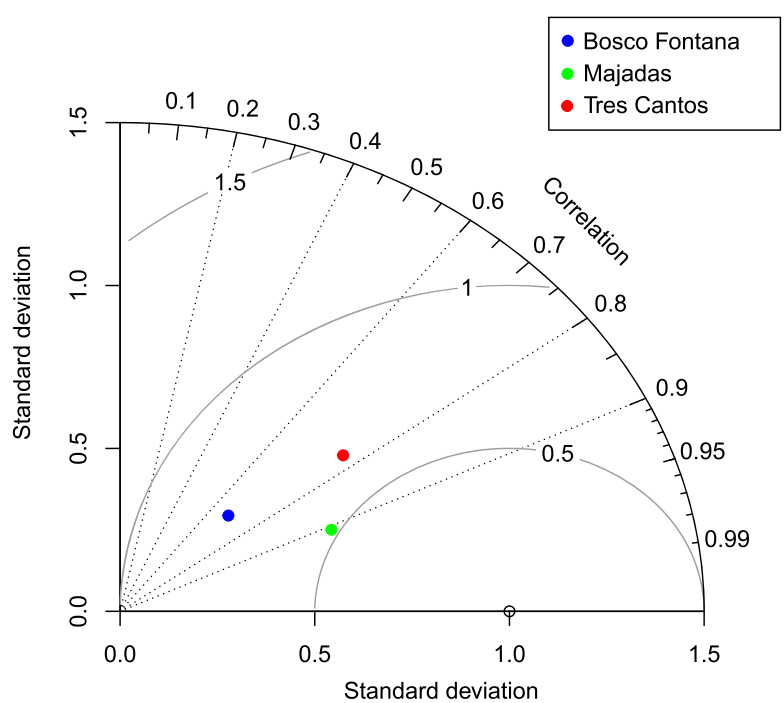

Fig. 2. Taylor diagram comparing the SMI modelled by ECMWF with the SMI measured at 30 cm for Bosco Fontana (Italy), at 40 cm for Majadas (Spain) and at 50 cm for Tres Cantos (Spain). Normalized standard deviation, correlation and centered root mean square difference are plotted to compare modelled and observed values between sites.

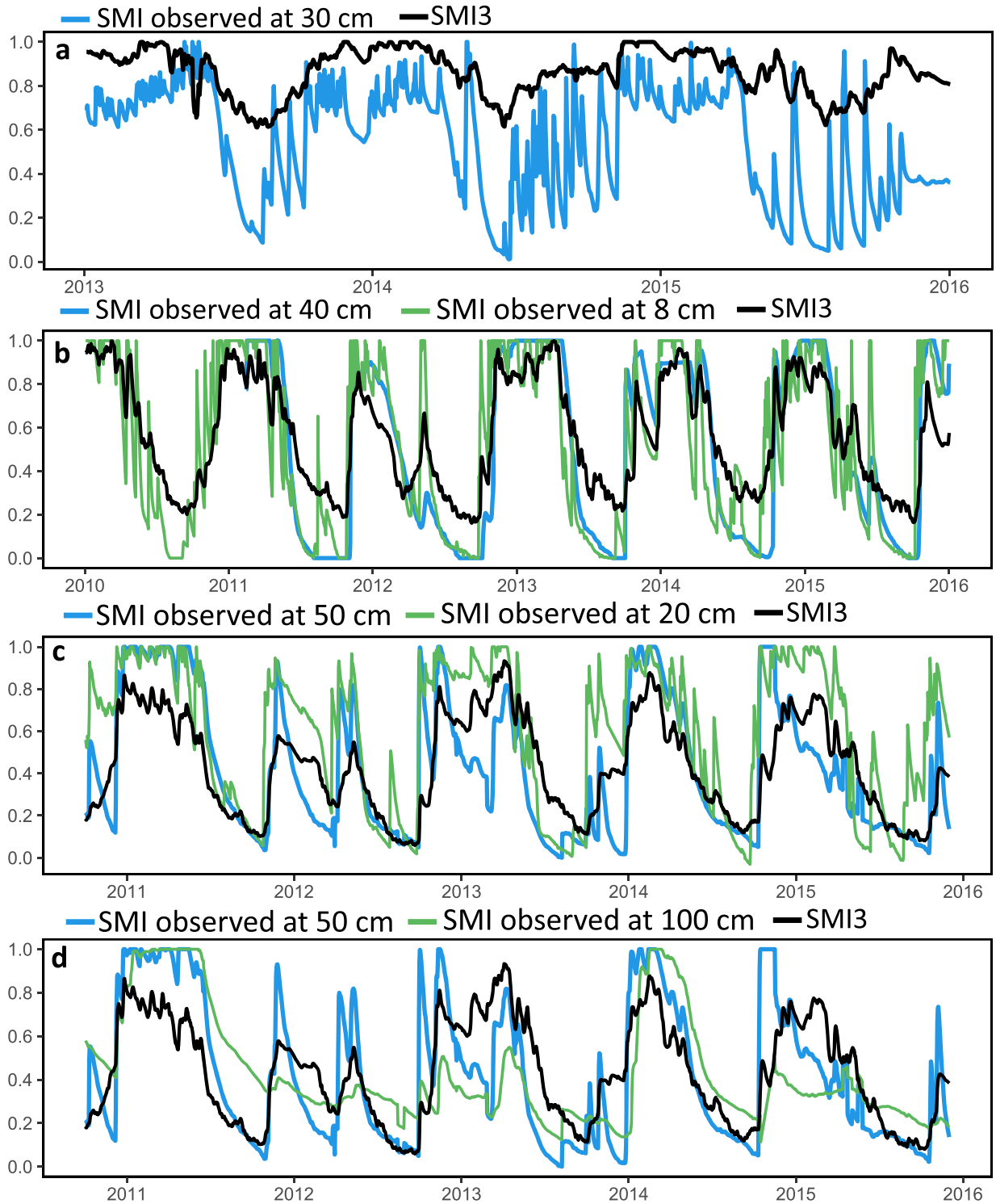

Fig. 3. SMI time series between 2010 and 2015 for a) Bosco Fontana (Italy) b) Majadas (Spain) c) sensor located in annual pastures in Tres Cantos (Spain) and d) sensor located in holm oak in Tres Cantos (Spain). The blue line represents the SMI observed at a) 30 cm b) 40 cm and c) 50 cm and d) 50 cm compared to the SMI observed at different depths in green b) 8 cm c) 20 cm and d) 100 cm. The black line represents the modelled SMI product (SMI3) of the ECMWF hydrological module H-TESSEL.

Core Team, 2022; Fox and Weisberg, 2019) in R to determine the sensitivity of *Q.ilex* soil moisture parametrizations to g_s measuring techniques, soil textures and soil depths, and to determine whether the parametrizations for Mediterranean annual pasture functional types differ significantly from each other. An analysis of variance (ANOVA) was conducted to compare these different f_{SMI} and f_{SWP} parametrizations between categories or functional types, followed by a post-hoc Bonferroni test. Shapiro-Wilk and Levene tests were performed to verify the normality and homoscedasticity assumptions for the ANOVA. A p-value below 0.05 was considered statistically significant in all tests. All statistical analyses were conducted using R and RStudio software version 4.2.1 and 2023.06.2, respectively (R core team, 2022).

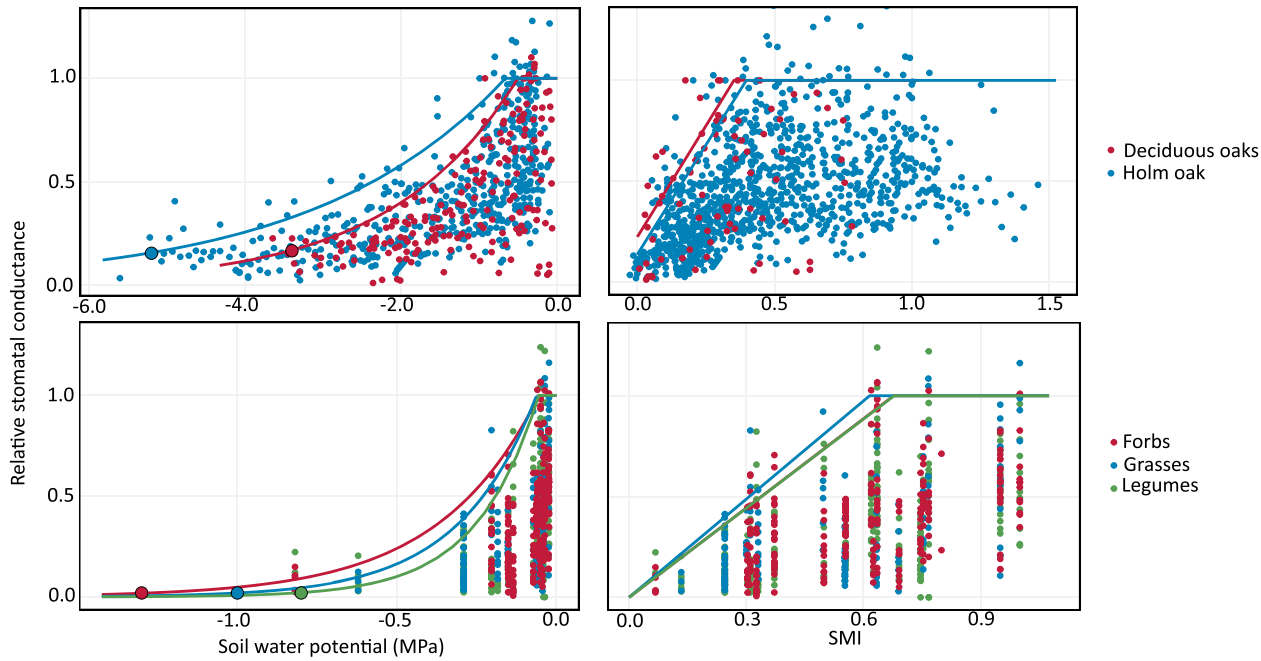

Fig. 4. Parametrization of f_{SWP} (left) and f_{SMI} (right) functions for holm oak (top blue), Mediterranean deciduous oak species (top red), forbs (bottom red), grasses (bottom blue) and legumes (bottom green). The SMI function of forbs coincides with that of legumes.

3. Results

3.1. Comparisons between modelled and observed SMI values

The comparison between observed and modelled SMI3 values in the 28–100 cm soil layer at the three field sites showed that SMI3 was responsive to the variability among sites, years and seasons (Figs. 2, 3 and A1). As a general pattern, SMI3 modelled values were closer to observations in MJD ($E = 0.521$), followed by TC ($E = 0.647$) and BF ($E = 0.779$) with a tendency to overestimate observed soil moisture, particularly at BF. The modelled values for BF suggest the absence of water limitation during the period analysed, although the observations showed more notable fluctuations, with some periods of very low water availability (Fig. 3).

The statistics represented in the Taylor diagram of Fig. 2 can be also found for sites, years, seasons and months (Tables A3-A6). Wetter years (2013 and 2014 in BF and 2011 and 2014 in MJD and TC) and autumn-winter season generally showed a better agreement between observed and modelled values (Figure A1), particularly in the Spanish drier sites, where greater variability in precipitation among years and seasons was found during the study period. The results observed on a monthly basis revealed more variations (Figure A2), with the best results for BF and TC found in December, November and January, while for MJD, the most favorable results were obtained in February, March and April. In MJD, the results for September have been excluded from Figure A2 for clarity. Results are affected by low observed and modelled SMI with low standard deviation and correlation coefficient, leading to high E values, standing out distinctly from other months.

3.2. f_{SMI} and f_{SWP} parametrizations

Fig. 4 presents the newly fitted f_{SWP} and f_{SMI} for Mediterranean broadleaf evergreen and deciduous forest species and for different Mediterranean annual pasture functional types (legumes, grasses and forbs) derived with boundary line analysis based on literature and field data of g_s collated in this study. More detailed figures are presented in the Supplementary Material (Figures A3-A7), showing the number of studies used for the SMI and SWP parametrization in forest species, as well as the data pertaining to each field site in annual pastures. The parameters derived from the boundary line analysis (SMI_{crit}, SWP_{max} and SWP_{min}) and the fit coefficients are presented in Table 2, together with the R correlation coefficient and the p-values.

Comparing forest species, the SWP boundary lines showed that *Q.ilex* was able to sustain higher g_s under decreasing water potentials compared to deciduous oaks ($p < 0.01$), which was reflected by more negative SWP_{max} and SWP_{min} values (Table 2). The soil moisture limiting functions based on the SMI, however, showed a very close response to soil drying between both forest species categories ($p = 0.948$). SMI_{crit} values, pointing the start of the water limiting stage to g_s, showed thus a remarkable similarity (Table 2).

Table 2
Summary of the linear and exponential fits of SMI and SWP functions, critical SMI (SMI_{crit}) and maximum and minimum SWP values (SWP_{max}, SWP_{min}) in MPa for Mediterranean evergreen forest species represented by holm oak, Mediterranean deciduous forest species represented by deciduous oaks and annual pastures functional types (legumes, grasses and forbs). R is the correlation coefficient and p is the p value.

			$r_{gs} = \min(1; a + b*SMI)$					$r_{gs} = \min(1; a*\exp(b*SWP))$					
			SMI_{crit}	a	b	R	p	SWP_{max}(MPa)	SWP_{min}(MPa)	a	b	R	p
Trees	Evergreen	*Quercus ilex*	0.4	0.137	2.175	0.927	<0.0001	−0.7	−5.2	1.311	0.407	0.973	<0.0001
	Deciduous	Deciduous oaks	0.4	0.224	2.207	0.829	<0.01	−0.5	−3.4	1.362	0.612	0.981	<0.0001
	Functional types	Legumes	0.7	0.000	1.474	0.986	<0.0001	−0.1	−0.8	1.329	5.144	0.960	<0.01
Annual pastures		Grasses	0.6	0.000	1.624	0.959	<0.001	−0.1	−1.0	1.241	4.129	0.996	<0.001
		Forbs	0.7	0.000	1.477	0.971	<0.0001	−0.1	−1.3	1.193	3.201	0.996	<0.01

Regression analyses performed by ANOVA showed differences in holm oak SWP functions fitted for different studies grouped by soil texture and soil depth (all $p < 0.01$, Figure A8). Holm oak trees reached more negative potentials in silty clay loam and deep soils (−4.9 and −4.2 MPa, respectively) than in clay loam and shallow soils (−3.0 MPa in both cases). Maximum g_s was kept at lower SWP in silty clay loam soils and in deep soils (−0.6 MPa and −0.8 MPa, respectively) compared to clay loam and shallow soils (−0.2 and −0.3 MPa, respectively). Differences were also found among g_s techniques ($p < 0.001$, Figure A8). A Bonferroni post-hoc analysis detected that, while the curve describing the eddy covariance data did not differ from leaf level measurements, both differed from the sapflow boundary line. Sapflow data showed g_s closing earlier (−0.3 MPa) than in eddy covariance (−0.6 MPa) or IRGA/porometer at the leaf level (−0.7 MPa) studies. In contrast, the regression analysis of f_{SMI} indicated no variability between soil textures ($p = 0.188$), depths ($p = 0.811$) and g_s measurement techniques ($p = 0.809$), as seen on the right side of Figure A8. The values of SMI_{crit}, SWP_{max}, and SWP_{min} calculated for each category in the sensitivity analysis of holm oak are outlined in Table A7. Althougth f_{SWP} parametrizations differed between g_s observation techniques, soil textures and soil depths, all available datasets for holm oak were considered to develop a general soil moisture limitation function.

f_{SMI} and f_{SWP} boundary lines for the annual pastures functional types studied are shown in the lower part of Fig. 4, where the f_{SMI} of forbs coincides with that of legumes. The f_{SWP} regression analysis identified statistically significant differences ($p < 0.001$) in annual pastures responses between legumes and grasses, as well as between legumes and forbs. All functional types of annual pastures began to close stomata at a SWP_{max} of −0.1 MPa (Table 2), which marks the point where g_s starts decreasing from its maximum value of 1. Forbs were able to reach a more negative potential (−1.3 MPa) than either grasses (−1.0 MPa) or legumes (−0.8 MPa) when g_{min} was reached. Conversely, no significant distinctions were observed among SMI functions ($p = 0.874$).

The new f_{SMI} and f_{SWP} parametrizations developed for holm oak and

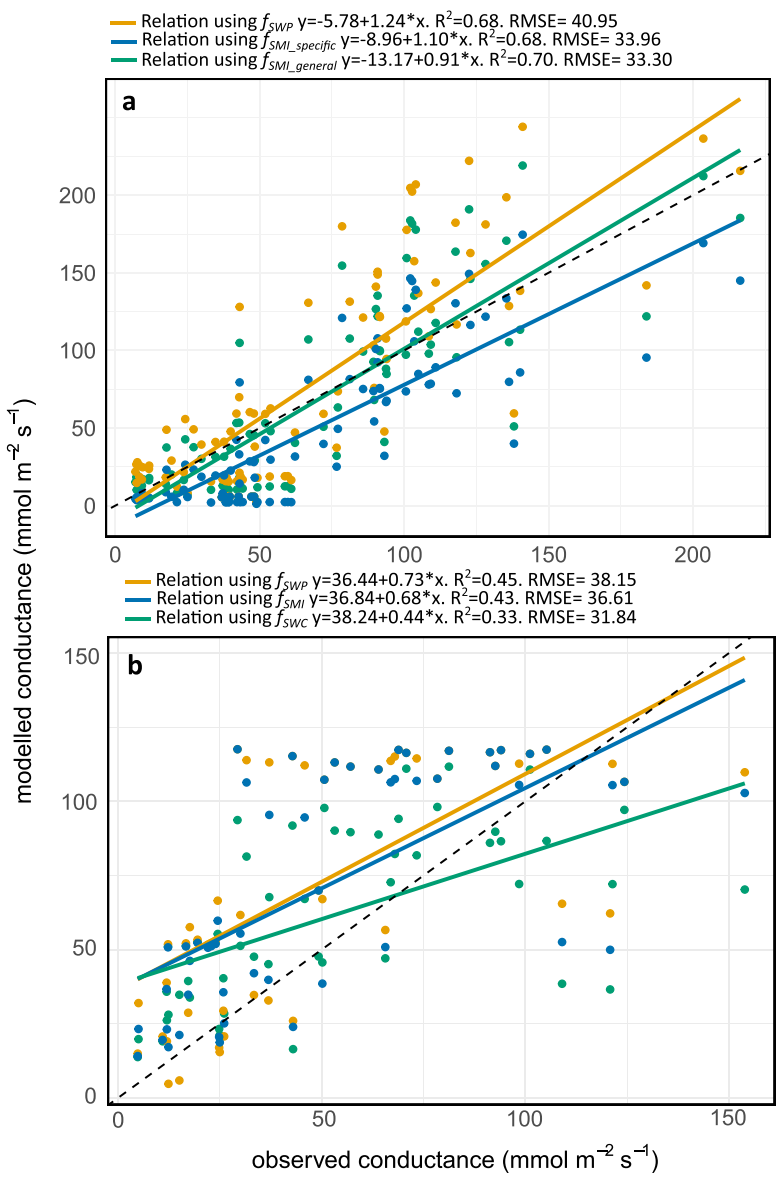

Fig. 5. Linear relationships between observed and modelled stomatal conductance (mmol m^{-2} s^{-1}) for a) holm oak and b) legume species. The equation and the squared correlation coefficient are presented to assess the model fit quality. The dashed line represents the line 1:1, where the observed and modelled stomatal conductance would have the same value. a) The holm oak SMI and SWP functions developed in this paper (f_{SWP} and $f_{SMI\_specific}$) and the standard SMI parametrization for all species ($f_{SMI\_general}$) were used to calculate the modelled stomatal conductance. The data used come from two locations in Spain: Miraflores and El Pardo. b) For legumes, specific SWP, SMI and SWC functions have been used with the data from Miraflores, Tres Cantos and Viñuelas (Spain).

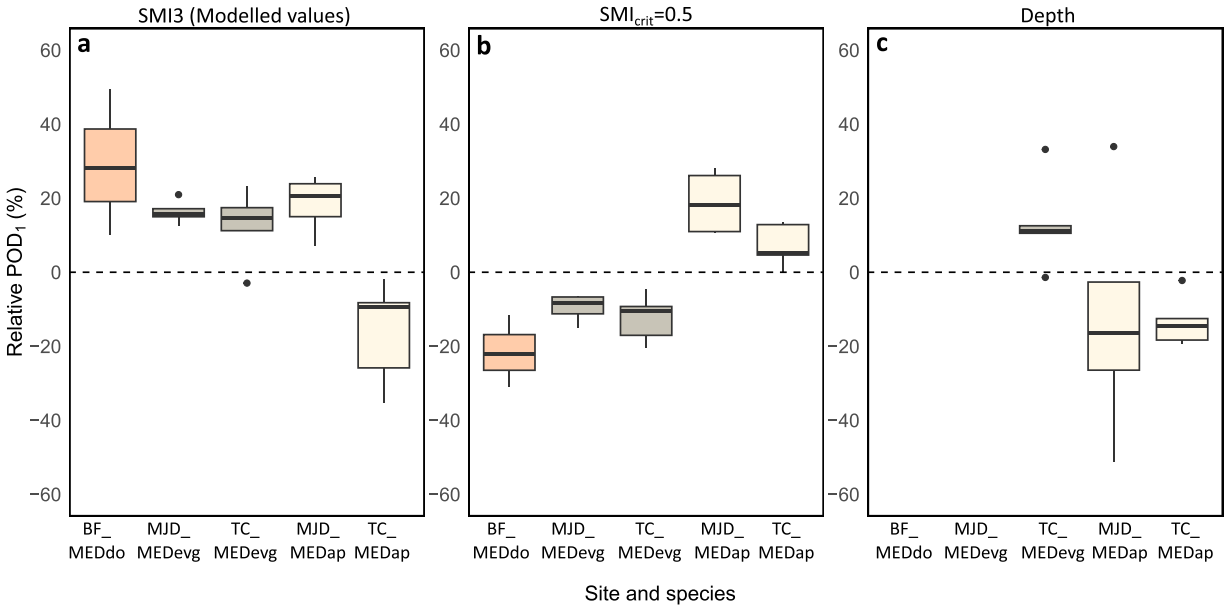

Fig. 6. Measured POD_1, expressed in relative terms (%), with respect to the POD_1 found with the different species-specific SMI functions for three locations (Bosco Fontana, BF; Majadas, MJD; Tres Cantos, TC) and three vegetation types (deciduous oaks in orange, holm oak in grey and annual pastures in light yellow). In BF, deciduous oaks are studied (labeled as BF_MEDdo), while in MJD and TC, both holm oak (MJD_MEDevg and TC_MEDevg) and annual pastures (MJD_MEDap and TC_MEDap) are addressed. The effect of (a) using modelled SMI3 instead of observed SMI values, (b) applying a general default parametrization with a fixed SMI_{crit} of 0.5 for all species, and (c) varying soil depths is tested. In the graph c, the impact of varying the depth from 40 cm to 8 cm for MJD_MEDap, from 50 cm to 100 cm for TC_MEDevg and from 50 cm to 20 cm in TC_MEDap is evaluated. Positive values indicate an overestimation of POD_1, while negative values suggest an underestimation. The black dotted line at 0 represents the point where both compared values are equal.

for the functional type legumes were used to model g_s and to compare it with measured values under field conditions. Similar g_s values have been obtained using the specific f_{SMI} or f_{SWP} (R^2 for both is 0.68) in holm oak (Fig. 5a), although the SMI fit was more similar to the 1:1 line and had a lower RMSE (33.96 mmol m^{-2} s^{-1}) than using SWP (40.95 mmol m^{-2} s^{-1}). The default general SMI parametrization (SMI_{crit}=0.5) tended to underestimate observed g_s (R^2=0.70 and RMSE=33.30 mmol m^{-2} s^{-1}), as it indicates that stomata close earlier than with the species-specific parametrization.

For the *Trifolium* data (Fig. 5b), the new f_{SMI} and f_{SWP} tended to overestimate g_s observations over most of the range, resulting in RMSE of 36.61 and 38.15 mmol m^{-2} s^{-1} respectively. These functions slightly improved the estimation of g_s compared with the previous soil moisture function based on SWC in terms of linear regression slope close to unity and lower RMSE of 31.84 mmol m^{-2} s^{-1}.

3.3. POD_1 calculations at field sites

POD_1 was calculated with SMI observations in the 28–100 cm depth soil layer with the f_{SMI} species-specific parametrizations developed in this study for the three field studies and main vegetation types at each site, establishing it as the best estimate of POD_1 when using SMI data (POD_1-SMI). Fig. 6 tests the effect of (a) using modelled SMI3 values instead of observed values; (b) using the default general parametrization for all species (where SMI_{crit}=0.5) instead of a species-specific one; and, (c) using SMI values observed at different depths in MJD and TC on the calculation of POD_1. All values are expressed in relative terms with respect to POD_1-SMI (in %). The impact of varying soil depth is assessed differently depending on the species: for annual pastures, POD_1 values were calculated using soil moisture sensors at <28 cm depth at each site (8 cm in MJD and 20 cm in TC); for holm oak, POD_1 was calculated using the 100 cm depth soil moisture records only in TC.

When modelled SMI3 values were used instead of observed SMI values (Fig. 6a), increases of 21 % on average were observed for forest species, but with large interannual variability, particularly in BF, depending on rainfall patterns and variability across years. In BF, where 2 very wet years (2013 and 2014) and one very dry year (2015) were considered, the greatest POD_1 increase (49 %) was found for the driest year. The extreme low relative POD_1 value in TC_MEDevg was caused by a wet growing season in 2011 (Fig. 3d). Despite lower modelled SMI3 values than observations that year, both variables showed non-limiting soil moisture availability for holm oak during most of the growing season, resulting in marginal differences in POD_1 estimation. For annual pastures, SMI3 resulted in POD_1 overestimation by 18 % on average in MJD but 16 % underestimation on average in TC. This outcome is a consequence of higher observed SMI values at 50 cm in TC than modelled SMI3 during the spring (Fig. 3c), when annual pastures are most actively growing and the POD_1 is calculated to estimate the risk of O_3 effect in this kind of vegetation.

Using the default general f_{SMI} parametrization underestimated POD_1 by 11 % and 22 % on average for Mediterranean evergreen and deciduous oak species, respectively, as a result of using a more restrictive SMI_{crit} of 0.5 compared with the species-specific parametrizations. The opposite occurred with the annual pastures in MJD and TC, where POD_1 found with the default parametrization produced an increase of 14 % on average, ranging up to 28 % overestimation, due to less restrictive SMI_{crit} in the default parametrization compared with the species-specific one.

The variation from 50 cm to 100 cm in the depth at which soil moisture is considered for POD_1 calculation for evergreen species, implied an increase of POD_1 by 13 % on average in TC_MEDevg. In 2013, TC_MEDevg exhibited a 1 % reduction in POD_1, in contrast to an average increase of 17 % observed in other years as a result of increasing the depth of soil moisture observations. This decline was attributed to consecutive dry years, which hindered the recharge of deeper soil layers (Fig. 3d). On the other hand, reductions of 21 % on average were observed for the annual pastures of MJD (from 40 cm to 8 cm) and TC (from 50 cm to 20 cm). In the MJD_MEDap results, an outlier was observed in the year 2012, leading to a 34 % increase in POD_1. This increase was attributed to higher SMI values at 8 cm compared to 40 cm (Fig. 3b) caused by an extended drought period during which rainfall was not able to replenish soil moisture storage capacity but in the most

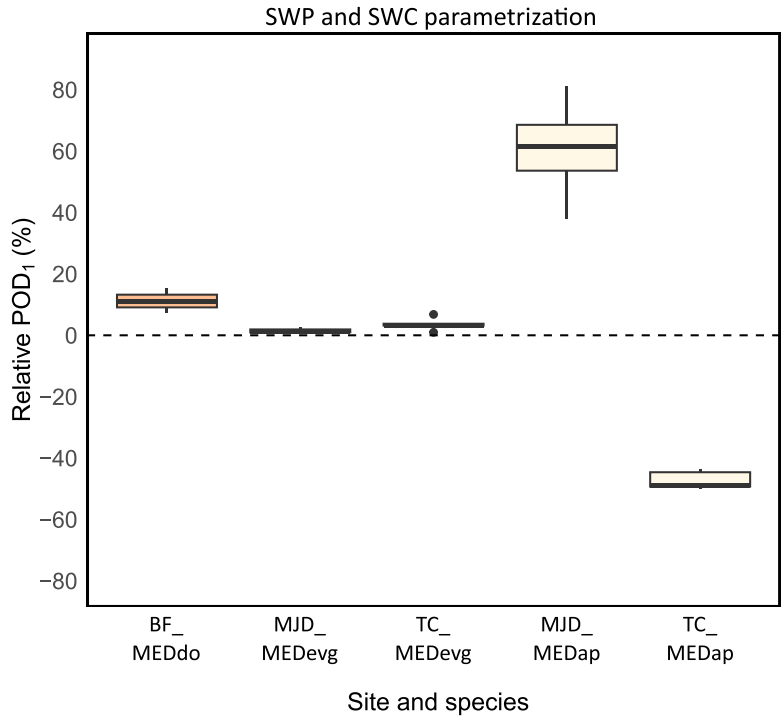

Fig. 7. POD_1 using the soil moisture parametrization already available in the Mapping Manual expressed in relative terms (%) with respect to POD_1 using the species-specific new SWP functions derived in this study for three sites (Bosco Fontana, BF; Majadas, MJD; Tres Cantos, TC) and three vegetation types (holm oak, deciduous oaks in orange and annual pastures in light yellow). In BF, the primary focus is on deciduous oaks (labeled as BF_MEDdo), while both holm oak forests (MJD_MEDevg and TC_MEDevg) and annual pastures (MJD_MEDap and TC_MEDap) are addressed in MJD and TC. For forest species, the effect of employing the Mapping Manual parametrization (with a linear form) is assessed in comparison to the species-specific parametrization with an exponential form developed in this study (with the new SWP_{max} and SWP_{min} parameters). Concerning annual pastures, the effect of using the soil water content (SWC) function from the Mapping Manual is evaluated in contrast to the function developed in this study by functional types (using legume species parametrization) with an exponential form. Positive values indicate an overestimation of POD_1, while negative values suggest an underestimation. The black dotted line at 0 represents the point where both compared values are equal.

superficial soil layer.

POD_1 was also calculated with SWP data using the f_{SWP} species-specific parametrizations developed in this study, establishing it as the best option when using SWP data (POD_1-SWP). Fig. 7 for forest species tests the effect of using the f_{SWP} parametrization of the Mapping Manual (changing the shape from exponential to linear as well as the SWP_{max} and SWP_{min} values), expressing it in relative terms (in %) with respect to POD_1-SWP. For annual pastures (Fig. 7), the effect of using f_{SWC} from the Mapping Manual with respect to POD_1-SWP is tested.

The use of the Mapping Manual f_{SWP} parametrization for holm oak resulted in an average 3 % overestimation in POD_1 in MJD and TC, and up to 7 % under the driest conditions considered in this study (Fig. 7). POD_1 was overestimated by 11 % for deciduous oaks in BF compared to employing the new f_{SWP} parametrization. For annual pastures, the use of the existing f_{SWC} function compared to the f_{SWP} developed in this study, resulted, on average, in POD_1 increases of 61 % in MJD and a decrease of 47 % in TC (Fig. 7).

4. Discussion

Soil moisture plays a significant role in influencing atmospheric O_3 concentrations through impacting the activity of vegetation and the exchange of O_3 and its precursors between the surface and the atmosphere (Domec et al., 2010; Val Martin et al., 2014; Lin et al., 2020; Yue et al., 2021). Drought conditions can induce leaf stomatal closure, which protects plants from excessive water loss and reduces the vegetation capacity to absorb O_3, resulting in higher atmospheric O_3 concentrations (Anav et al., 2018; Lin et al., 2020). Reduced rates of stomatal uptake also lower the risk of O_3 negative effects on plant physiology (Fagnano and Maggio, 2018; Kask et al., 2021), although it may not result in full protection against O_3 injury (Alonso et al., 2014). In agreement with its importance, atmospheric chemistry models and O_3 risk assessment methodologies include soil moisture among their driving variables (Büker et al., 2012; Simpson et al., 2012; Anav et al., 2018) using metrics like the SMI. However, although some efforts have been made to evaluate the EMEP model's estimates of ozone fluxes and POD_y values (Tuovinen et al., 2004; Klingberg et al., 2008), most datasets were from temperate/boreal ecosystems, and the formulation of the SMI-g_s-POD_y relationships has not been tested in southern Europe before.

The evaluation of modelled (SMI3) and observed SMI values at the three field sites considered in this study is consistent with previous soil moisture validation exercises with independent soil moisture databases (Albergel et al., 2012b; Gao et al., 2016), showing that SMI can be used to represent soil moisture variations across sites, years and seasons. However, a higher similarity between modelled and observed SMI was obtained at the site with intermediate precipitation conditions (MJD) compared to the drier and wetter sites (TC and BF, respectively). Modelled SMI3 was also more accurate in wetter years and seasons, especially in autumn and winter and, overall, there was a tendency to overestimate soil moisture under drought conditions. As a result, using modelled SMI3 values for representing soil moisture dynamics resulted in a 20 % overestimation of POD_1 on average (except for the case of TC_MEDap, annual pastures at TC site) compared with calculations based on observed SMI values. The largest overestimates when considering the full set of years occurred in BF, as well as in the dry years of the three sites considered. The different behavior of SMI3 among sites could be related to variations in soil and vegetation properties that may not be fully captured by the SMI3 values, partly because of the coarser resolution of SMI3 (IFS model takes the predominant soil texture among 6 available classes of each nominal 10 km resolution cell), as soil texture is a highly spatially variable property (Liao et al., 2013; Paterson et al., 2018). These results show that, although the consideration of these

parametrizations are a big improvement for POD_y estimation, a considerable source of uncertainty remains for years and sites subject to great water scarcity.

Differences between modelled and observed SMI could also arise from plant species ability to extract soil water, which is known to vary among species (Schwendenmann et al., 2015; Brinkmann et al., 2019). Plant species follow different strategies regarding water use, from water saving through to water stress avoidance or tolerance, showing a wide range of adaption traits that result in differences in plant water status and stomatal control level (Chaves et al., 2002; Osakabe et al., 2014). The analysis of the g_s response to predawn LWP showed that holm oak was able to sustain higher g_s under increasing water stress and reach lower LWP values compared to deciduous Mediterranean oak species. This result is consistent with their different strategies to cope with water stress reported in the literature (Salleo and Gullo, 1990; Acherar and Rambal, 1992; Alonso-Forn et al., 2021). The f_{SWP} functions for Mediterranean tree species also showed a greater tolerance to decreasing SWP than central and northern European tree species (Norway spruce, Scots pine and beech) reported in Büker et al. (2012). Annual pasture functional types exhibited a distinct f_{SWP} and f_{SMI} compared to forest trees, consistent with their therophytic growing habit and stress-avoidance strategy (Socias et al., 1997; Guàrdia et al., 1998; Kostopoulou et al., 2010), closing stomata at higher SWP and SMI values compared to holm oak trees sharing the same habitat. Among pasture species, differences in f_{SWP} were also found between functional types, particularly between legumes and grasses and between grasses and forbs. The SWP_{min} values obtained for the annual pastures functional types are less negative than those reported in pots for related species, ranging from −1 MPa to −2.9 MPa (Aparicio-Tejo et al., 1980; Galmés et al., 2007; Karatassiou et al., 2009; Kostopoulou et al., 2010). One potential explanation for this variation may be attributed to uncertainties in the conversion of SWC to SWP in the generation of f_{SWP} curves. This process involves the utilization of the van Genuchten model to compute SWP values, along with the acquisition of necessary soil hydraulic parameters through pedotransfer functions, which introduce a source of uncertainty into the determination of SWP. Also, the estimation of the SWP_{min} parameter for annual pasture functional types was limited by the scarcity of measurements under low soil moisture availability. Future measurements under field conditions should be performed to directly estimate the relationships between predawn LWP and g_s in these species. In general, all these results highlight that the g_s relationship with soil moisture is species-specific and should be adequately parameterized for improving POD_y modelling exercises.

Apart from species-specific differences, leaf water potential is also modified by soil properties, plant physiology, vegetation density or land use (Bréda et al., 1995; Montero et al., 2004; Bhaskar and Ackerly, 2006). In fact, differences in physiological and g_s responses to decreasing LWP or soil moisture have been found within the same species (Rambal et al., 2003; Bolte et al., 2016). In agreement with this, regression analyses of f_{SWP} functions for holm oak showed differences depending on soil texture and soil depth categories. These results suggests that locally derived f_{SWP} may be more appropriate for describing g_s responses to soil moisture and estimating POD_y at the plot scale. However, since site-specific information is sometimes fragmentary and difficult to collect, species-specific f_{SWP} are also proposed in this study for use in g_s and POD_y modelling and in O_3 risk assessment at larger scales. The influence of different techniques for g_s determination under field conditions on f_{SWP} was also tested for holm oak: while IRGA/porometer at the leaf level and eddy covariance resulted in comparable f_{SWP}, the sapflow study yielded a different result. This should warn against combining field data obtained using different methodologies, although this comparison was limited to a single study and did not modify the general f_{SWP}. Similar comparisons for other species were not possible due to insufficient data.

The newly developed f_{SWP} limiting functions represent an update, with the most recent literature and field data, of existing functions for evergreen and deciduous Mediterranean trees, while a new soil moisture function using SWP is proposed for Mediterranean annual pasture functional types (Büker et al., 2012; CLRTAP, 2017). The use of the Mapping Manual f_{SWP} parametrization results in less than 5% variations on average in POD_1 for forest trees (higher in deciduous oaks, 11 % on average) under the growing conditions evaluated in the present study (Fig. 7). Although the data indicate an exponential response of g_s to decreasing SWP, changing the form of the function from linear to exponential as well as the SWP_{min} and SWP_{max} parameters did not have a large effect, although this effect was greater in the drier years, for the sites and conditions considered in this study. On the other hand, greater variations were found when testing the effect of existing parametrizations used in O_3 risk assessment methodologies for annual pastures based on SWC, with respect to the parametrizations developed in this study. This result was affected by the strong influence of local physico-chemical soil properties of the field studies used to derive f_{SWC} that resulted in large POD_1 differences between MJD and TC. SWC values in MJD frequently exceeded SWC_{max} value of the existing parametrization while SWC in TC remained always under this value because of a lower field capacity at that site. Therefore, it is recommended to use f_{SWP} in the estimation of POD_1 for annual pastures instead of f_{SWC}, as SWC is more dependent on soil texture.

The information gathered on g_s response to LWP or SWC was used to parameterize f_{SMI}, as the SMI is being used to estimate POD_y in the EMEP model (Simpson et al., 2012, 2022). The new f_{SMI} functions for Mediterranean forest and annual pasture species were used for g_s estimation and compared with field g_s measurements, showing a similar result compared with estimates based on f_{SWP} or f_{SWC} (Fig. 5b). New SMI_{crit} values, ranging from 0.4 to 0.7, induced changes in POD_1 estimation at the three field sites. The application of a default general parametrization leaded to an average reduction of 15 % in POD_1 for deciduous oaks and holm oak compared to the species-specific f_{SMI}. In contrast, an opposite effect was observed in annual pastures, where the use of a SMI_{crit} of 0.5 resulted in a mean increase of 14 % in POD_1 with respect to its species-specific parametrization.

The new SMI_{crit} values fall within the range of 0.2–0.8 fraction of PAW representing the start of soil moisture limitation to evapotranspiration or g_s reported for different species (Allen et al., 1998; Bréda et al., 1995; Sadras and Milroy, 1996). Interestingly, despite significant f_{SWP} differences were found among species, f_{SMI} and SMI_{crit} values were very similar between Mediterranean forest species. This result could be affected by the amount of SMI data available in each case ($n = 959$ for holm oak and $n = 73$ for deciduous oaks). Also, no variability was found in f_{SMI} due to differences in soil texture, soil depth or g_s measuring technique in studies with holm oak, in contrast with the result obtained with f_{SWP}. This result is probably caused by (i) the standardization of different species-specific SWP_{min} value to a common SMI of 0; (ii) the non-linear relationship between SWP and SWC, where large changes in low SWP values cause a small change in SWC and thus in SMI; and (iii), that SMI_{crit} values are related with SWP_{max} and there seem to be a smaller inter-specific variability in this particular parameter compared with SWP_{min} (Büker et al., 2012). This makes the SMI_{crit} a more robust parameter to varying site conditions (which is a good feature for large-scale modelling of POD_y) but less able to detect differences in soil moisture stress tolerance between plant species than SWP parameters. Another interesting finding is that the f_{SMI} for the Mediterranean forest species do not reach 0 when SMI=0, maintaining a certain level of g_s. This is in agreement with previous studies reporting partial stomatal opening even at very low LWP values (Rhizopoulou and Mitrakos, 1990; Rambal et al., 2003). This result suggests the need for including a second SMI parameter (SMI_{min}) in g_s parametrizations for POD_y estimation for representing this physiological response to soil moisture stress of some species.

The new f_{SWP} and f_{SMI} parametrizations proposed in this study were developed assuming that pre-dawn LWP is in equilibrium with SWP (Richter, 1997; Rambal et al., 2003). However, particularly in dry areas,

species may not have enough time to recover from the water losses occurring during the day and to equilibrate with the soil before dawn (Sellin, 1999; Donovan et al., 2001). This effect was not taken into account in the analyses presented here. Other sources of uncertainty lay in the method used to transform LWP into SWC (and the opposite in annual pastures) using the soil hydraulic properties of the van Genuchten model obtained from pedotranfer functions (Szabó et al., 2021) or maps of the European Soil Hydraulic Database (Tóth et al., 2017) when site-specific soil moisture retention curves were not available. In Montpellier (France) (Rambal et al., 2003; Limousin et al., 2009; Misson et al., 2010), the available information allowed to compare soil moisture retention curves from field data with soil hydraulic mapped properties and pedotransfer functions. The pedotransfer functions generated an outcome that closely resemble the maps from the European Soil Hydraulic Database, indicating an overestimation of the field water availability in both cases. In Tarragona (Spain) (Aguadé et al., 2015), the predictive capacity of maps concerning the soil moisture retention curve is notably limited. Furthermore, in Miraflores and El Pardo (Alonso et al., 2008), a comparative analysis between the pedotransfer functions and the maps demonstrated that the former yielded lower estimates of soil moisture content compared to those indicated by the maps.

The soil depth at which soil moisture is monitored appeared as one of the most relevant factors influencing g_s and POD_1 estimates at the field sites considered in this study. The EMEP model use the SMI3 index, representing the soil moisture in the 28–100 cm depth soil layer, for modelling soil moisture limitations to g_s for all vegetation species. However, some adapted forest species such as holm oak can develop roots with depths of approximately 4 to 5 m in sandy and sandstone soils, and a horizontal extension of 33 m in Spain (Canadell et al., 1996; Moreno et al., 2005). On the contrary, drought avoiding Mediterranean annual pastures species tend to develop shallow rooting systems, with roots laying mostly in the first 30 cm of soil, reaching a maximum rooting depth of 0.8 m (Schenk and Jackson, 2002; Moreno et al., 2005). In agreement with this, some studies have shown that trees take up water from deeper soil layers than herbaceous plants (Wang et al., 2020; Benegas et al., 2021), suggesting that species-specific rooting distributions and depth would be more appropriate to describe soil moisture limiting effects on g_s than using a single rooting depth for all species. Changing SMI observed values at 100 cm depth increased POD_1 for Mediterranean evergreen forest trees up to 13 % compared with SMI at 50 cm. For annual pastures, varying the depth to less than 28 cm (8 cm in MJD and 20 cm in TC) implied decreases in POD_1 of 21 % on average. In the year 2012, within the MJD_MEDap dataset, POD_1 exhibited higher levels considering soil moisture at 8 cm depth compared to 50 cm. This result was caused by higher water availability at 8 cm compared to 50 cm during a dry year. Similar soil moisture dynamics have been described in short grass steppes, where rainfall events during prolonged dry periods only moistened the most superficial soil layers, affecting ecosystem processes (Sala et al., 1992). Other studies have also shown the important influence of varying soil moisture with depth on POD_y modelling exercises (Anav et al., 2018; Büker et al., 2012).

More complex representations of the limiting effect of soil moisture on plant physiology take into account the chemical and hydraulic signalling, ensuring interactions within the entire system (Verhoef and Egea, 2014). However, their application is currently limited to situations where appropriate parametrizations are available since root distribution is influenced by multiple factors such as soil depth and texture, plant age, chemical conditions and even genetic material (Bréda et al., 1995; Czajkowski et al., 2009), and even presenting variations within the same soil texture (Sadras and Milroy, 1996). Future research should focus on incorporating rooting depth and root distribution parameters to enhance the evaluation of plant water status and soil moisture impacts on g_s and O_3 uptake.

5. Conclusions

The SMI, which is currently used in large scale atmospheric modelling studies, is an appropriate index to represent soil moisture variations across sites, years and seasons in Mediterranean areas. However, modelled SMI tends to overestimate plant water availability, particularly for the driest years and seasons, which might be related to a potential misrepresentation of soil characteristics at the local scale or to differences in vegetation traits related with water stress tolerance. To address this uncertainty, SWP limiting functions have been updated and new species-specific SMI limiting functions have been developed to model g_s, incorporating the latest available data. It is recommended to employ these newly SMI and SWP developed functions for estimating POD_y for Mediterranean species in future studies, and new parametrizations for other species should be developed. Limiting functions based on SWP are preferred for local scale applications, as they are able to reflect site-specific growing conditions affecting plant water status and are better at discriminating the drought tolerance of different species compared to SMI. Future work, however, should consider the species-specific parametrization of rooting depth and root distribution to enhance the assessment of plant water status and soil moisture limiting effects on g_s and O_3 uptake. These traits emerged among the most crucial factors affecting the POD_y estimation. Continued research in this field will contribute to refining risk assessment for vegetation associated with O_3 pollution, both under current conditions and in future climate change scenarios, where water limitation is expected to extend to more regions of Europe.

CRediT authorship contribution statement

Tania Carrasco-Molina: Writing – original draft, Visualization, Methodology, Investigation, Formal analysis, Conceptualization. **Riccardo Marzuoli:** Writing – review & editing, Investigation, Conceptualization. **Vicent Calatayud:** Writing – review & editing, Investigation, Conceptualization. **David Simpson:** Writing – review & editing, Investigation, Conceptualization. **Giacomo Gerosa:** Writing – review & editing, Investigation, Conceptualization. **Arnaud Carrara:** Writing – review & editing, Investigation. **Isaura Rábago:** Writing – review & editing, Funding acquisition, Conceptualization. **Rocío Alonso:** Writing – review & editing, Investigation, Conceptualization. **Ignacio :** Writing – review & editing, Supervision, Methodology, Investigation, Conceptualization.

Declaration of competing interest

The authors declare that they have no known competing financial interests or personal relationships that could have appeared to influence the work reported in this paper.

Data availability

Data will be made available on request.

Acknowledgments

Funding was provided by the following projects: DGCEA - CIEMAT working programme on atmospheric pollution and persistent organic pollutants (ACTUA-MITERD, Spanish Ministry of Ecological Transition); MITERD-SEMA-OAPN - CIEMAT working programme on air pollution monitoring and effects at the Spanish network of National Parks (RECAEPN, Organismo Autónomo Parques Nacionales, Spanish Ministry of Ecological Transition) – funded by NextGenerationEU/PRTR; Project TRANSAIRE: Transición hacia un aire más limpio en España (TED2021-132431B-I00) funded by MCIN/AEI /10.13039/501100011033 and NextGenerationEU/PRTR. Measurements at Tres Cantos monitoring site

was possible thanks to an agreement between CIEMAT and Ayuntamiento de Madrid. Measurements at BF were supported by the FP7 project ÉCLAIRE of the European Union, by the TREEcity project of primarian national interest of the Italian Ministry of University and Research, and by the Catholic University of the Sacred Heart. The authors thank the Forest Police (Carabinieri Forestali) and the personnel of the BF natural reserve for their help. VC and AC thank the support of projects ELEMENTAL (CGL2017-83538-C3-3-R), and URBFLUX (PID2021-125941OB-I00), funded by MCIN/AEI/ 10.13039/ 501100011033 and "ERDF A way of making Europe". The modelled SMI data were made available from the EMEP model infrastructure, which is supported by the EMEP Trust fund, as well as resources provided by UNINETT Sigma2 – the National Infrastructure for High Performance Computing and Data Storage in Norway (grant NN2890k and NS9005k)

Supplementary materials

Supplementary material associated with this article can be found, in the online version, at doi:10.1016/j.agrformet.2024.110080.

References

Acherar, M., Rambal, S., 1992. Comparative water relations of four Mediterranean oak species. Vegetatio (1), 99–100.
Agathokleous, E., Feng, Z., Oksanen, E., Sicard, P., Wang, Q., Saitanis, C.J., Araminiene, V., Blande, J.D., Hayes, F., Calatayud, V., Domingos, M., Veresoglou, S. D., Peñuelas, J., Wardle, D.A., de Marco, A., Li, Z., Harmens, H., Yuan, X., Vitale, M., Paoletti, E., 2020. Ozone affects plant, insect, and soil microbial communities: a threat to terrestrial ecosystems and biodiversity. Sci. Adv. 6 (33).
Aguadé, D., Poyatos, R., Rosas, T., Martínez-Vilalta, J., 2015. Comparative drought responses of Quercus ilex L. and Pinus sylvestris L. In a montane forest undergoing a vegetation shift. Forests 6 (8).
Albergel, C., de Rosnay, P., Balsamo, G., Isaksen, L., Muñoz-Sabater, J., 2012b. Soil moisture analyses at ECMWF: evaluation using global ground-based *in situ* observations. J. Hydrometeorol. 13 (5).
Albergel, C., de Rosnay, P., Balsamo, G., J, M.-S., Boussetta, S., Isaksen, L, 2012a. ECMWF soil moisture validation activities. ECMWF Newsletter. ECMWF, pp. 23–29. https://doi.org/10.21957/j3qge8l3.
Allen, R.G., Pereira, L.S., Raes, D., Smith, M., W, a B, 1998. Crop Evapotranspiration - Guidelines for Computing Crop Water Requirements - FAO Irrigation and Drainage Paper 56. Irrigation and Drainage.
Alonso, R., Bermejo, V., Sanz, J., Valls, B., Elvira, S., Gimeno, B.S., 2007a. Stomatal conductance of semi-natural Mediterranean grasslands: implications for the development of ozone critical levels. Environ. Pollut. 146 (3).
Alonso, R., Elvira, S., González-Fernández, I., Calvete, H., García-Gómez, H., Bermejo, V., 2014. Drought stress does not protect Quercus ilex L. from ozone effects: results from a comparative study of two subspecies differing in ozone sensitivity. Plant Biol. 16 (2).
Alonso, R., Elvira, S., Sanz, M.J., Emberson, L., Gimeno, B.S., 2007b. Parameterization of the stomatal component of the DO3SE model for Mediterranean evergreen broadleaf species. Sci. World J. 7 (SUPPL. 1), 119–127.
Alonso, R., Elvira, S., Sanz, M.J., Gerosa, G., Emberson, L.D., Bermejo, V., Gimeno, B.S., 2008. Sensitivity analysis of a parameterization of the stomatal component of the DO3SE model for Quercus ilex to estimate ozone fluxes. Environ. Pollut. 155 (3).
Alonso-Forn, D., Peguero-Pina, J.J., Ferrio, J.P., Mencuccini, M., Mendoza-Herrer, Ó., Sancho-Knapik, D., Gil-Pelegrín, E., 2021. Contrasting functional strategies following severe drought in two Mediterranean oaks with different leaf habit: quercus faginea and Quercus ilex subsp. rotundifolia. Tree Physiol. 41 (3).
Anav, A., Proietti, C., Menut, L., Carnicelli, S., de Marco, A., Paoletti, E., 2018. Sensitivity of stomatal conductance to soil moisture: implications for tropospheric ozone. Atmos. Chem. Phys. 18 (8).
Aparicio-Tejo, P.M., Sánchez-Díaz, M.F., Peña, J.I., 1980. Nitrogen fixation, stomatal response and transpiration in Medicago sativa, Trifolium repens and T. subterraneum under water stress and recovery. Physiol. Plant 48 (1), 1–4.
Aranda, I., Gil, L., Pardos, J.A., 2000. Water relations and gas exchange in Fagus sylvatica L. and Quercus petraea (Mattuschka) Liebl. in a mixed stand at their southern limit of distribution in Europe. Trees - Struct. Funct. 14 (6), 344–352.
Balsamo, G., Viterbo, P., Beijaars, A., van den Hurk, B., Hirschi, M., Betts, A.K., Scipal, K., 2009. A revised hydrology for the ECMWF model: verification from field site to terrestrial water storage and impact in the integrated forecast system. J. Hydrometeorol. 10 (3).
Benegas, L., Hasselquist, N., Bargués-Tobella, A., Malmer, A., Ilstedt, U., 2021. Positive effects of scattered trees on soil water dynamics in a pasture landscape in the tropics. Front Water 3.
Bhaskar, R., Ackerly, D.D., 2006. Ecological relevance of minimum seasonal water potentials. Physiol. Plant 127, 353–359.
Bolte, A., Czajkowski, T., Cocozza, C., Tognetti, R., de Miguel, M., Pšidová, E., Ditmarová, L., Dinca, L., Delzon, S., Cochard, H., Ræbild, A., de Luis, M., Cvjetkovic, B., Heiri, C., Müller, J., 2016. Desiccation and mortality dynamics in seedlings of different European beech (Fagus sylvatica L.) populations under extreme drought conditions. Front. Plant Sci. 7.
Bréda, N., Granier, A., Barataud, F., Moyne, C., 1995. Soil water dynamics in an oak stand. Plant Soil 172 (1).
Brinkmann, N., Eugster, W., Buchmann, N., Kahmen, A., 2019. Species-specific differences in water uptake depth of mature temperate trees vary with water availability in the soil. Plant Biol. 21 (1).
Büker, P., Morrissey, T., Briolat, A., Falk, R., Simpson, D., Tuovinen, J.P., Alonso, R., Barth, S., Baumgarten, M., Grulke, N., Karlsson, P.E., King, J., Lagergren, F., Matyssek, R., Nunn, A., Ogaya, R., Pëuelas, J., Rhea, L., Schaub, M., Emberson, L.D., 2012. DO_3SE modelling of soil moisture to determine ozone flux to forest trees. Atmos. Chem. Phys. 12 (12).
Calatayud, V., Cerveró, J., Calvo, E., García-Breijo, F.J., Reig-Arminana, J., Sanz, M.J., 2011. Responses of evergreen and deciduous Quercus species to enhanced ozone levels. Environ. Pollut. 159 (1).
Calvete-Sogo, H., Elvira, S., Sanz, J., González-Fernández, I., García-Gómez, H., Sánchez-Martín, L., Alonso, R., Bermejo-Bermejo, V., 2014. Current ozone levels threaten gross primary production and yield of Mediterranean annual pastures and nitrogen modulates the response. Atmos Environ 95.
Canadell, J., Jackson, R.B., Ehleringer, J.R., Mooney, H.A., Sala, O.E., Schulze, E.D., 1996. Maximum rooting depth of vegetation types at the global scale. Oecologia 108 (4).
Carslaw, D.C., Ropkins, K., 2012. Openair - an r package for air quality data analysis. Environ. Modell. Softw. 27–28. https://doi.org/10.1016/j.envsoft.2011.09.008.
Castagna, A., Ranieri, A., 2009. Detoxification and repair process of ozone injury: from O3 uptake to gene expression adjustment. Environ. Pollut. 157 (5).
Castell, C., Terradas, J., Tenhunen, J.D., 1994. Water relations, gas exchange, and growth of resprouts and mature plant shoots of Arbutus unedo L. and Quercus ilex L. Oecologia 98 (2).
Chambers, J.L., Hinckley, T.M., Cox, G.S., Metcalf, C.L., Aslin, R.G., 1985. Boundary-line analysis and models of leaf conductance for four oak-hickory forest species. Forest Sci. 31 (2).
Chaves, M.M., Pereira, J.S., Maroco, J., Rodrigues, M.L., Ricardo, C.P.P., Osório, M.L., Carvalho, I., Faria, T., Pinheiro, C., 2002. How plants cope with water stress in the field. Photosynthesis and growth. Ann. Bot. 89 (SPEC. ISS.).
CLRTAP, 2017. Mapping Critical Levels For Vegetation, Chapter III. Manual on Methodologies and Criteria for Modelling and Mapping Critical Loads and Levels and Air Pollution Effects, Risks and Trends. Convention on Long-Range Transboundary Air Pollution.
Czajkowski, T., Ahrends, B., Bolte, A., 2009. Critical limits of soil water availability (CLSWA) for forest trees - an approach based on plant water status. Landbauforschung Volkenrode 59 (2).
Dafka, S., Akritidis, D., Zanis, P., Pozzer, A., Xoplaki, E., Luterbacher, J., Zerefos, C., 2021. On the link between the Etesian winds, tropopause folds and tropospheric ozone over the Eastern Mediterranean during summer. Atmos. Res. 248.
Damesin, C., Rambal, S., 1995. Field study of leaf photosynthetic performance by a Mediterranean deciduous oak tree (Quercus pubescens) during a severe summer drought. New Phytol. 131 (2), 159–167.
Diaz-de-Quijano, M., Kefauver, S., Ogaya, R., Vollenweider, P., Ribas, À., Peñuelas, J., 2016. Visible ozone-like injury, defoliation, and mortality in two Pinus uncinata stands in the Catalan Pyrenees (NE Spain). Eur. J. For. Res. 135 (4).
Domec, J.C., King, J.S., Noormets, A., Treasure, E., Gavazzi, M.J., Sun, G., McNulty, S.G., 2010. Hydraulic redistribution of soil water by roots affects whole-stand evapotranspiration and net ecosystem carbon exchange. New Phytol. 187 (1).
Donovan, L., Linton, M., Richards, J., 2001. Predawn plant water potential does not necessarily equilibrate with soil water potential under well-watered conditions. Oecologia 129 (3).
ECMWF, 2021b. Change to Soil Hydrology Scheme in IFS cycle 32r3. https://www.ecmwf.int/en/forecasts/documentation-and-support/evolution-ifs/cycles/change-soil-hydrology-scheme-ifs-cycle (last Accessed November 2023).
ECMWF, 2021a. IFS Documentation CY47R3 - Part IV physical processes. IFS Documentation CY47R3. ECMWF. https://doi.org/10.21957/eyrpir4vj.
El-Madany, T.S., Reichstein, M., Perez-Priego, O., Carrara, A., Moreno, G., Pilar Martin, M., et al., 2018. Drivers of spatio-temporal variability of carbon dioxide and energy fluxes in a Mediterranean savanna ecosystem. Agric. For. Meteorol. 262.
Emberson, L., 2020. Effects of ozone on agriculture, forests and grasslands. Philos. Trans. R. Soc. A 378 (2183).
Emberson, L.D., Ashmore, M.R., Cambridge, H.M., Simpson, D., Tuovinen, J.P., 2000. Modelling stomatal ozone flux across Europe. Environ. Pollut. 109 (3).
Emberson, L.D., Ashmore, M.R., Simpson, D., Tuovinen, J.P., Cambridge, H.M., 2001. Modelling and mapping ozone deposition in Europe. Water Air Soil Pollut. 130, 1-4 II.
European Environment Agency, 2023. Europe's Air Quality Status 2023.
Fagnano, M., Maggio, A., 2018. On the interactions among tropospheric ozone levels and typical environmental stresses challenging Mediterranean crops. Environ. Sci. Pollut. Res. 25 (9).
Filho, J.T., Damesin, C., Rambal, S., Joffre, R., 1998. Retrieving leaf conductances from sap flows in a mixed Mediterranean woodland: a scaling exercise. Annal. Sci. Forest. 55 (1–2).
Forner, A., Valladares, F., Aranda, I., 2018. Mediterranean trees coping with severe drought: avoidance might not be safe. Environ. Exp. Bot. 155.
Fox, J., Weisberg, S., 2019. An {R} Companion to Applied Regression, 3rd ed. Sage, Thousand Oaks CA.
Fuhrer, J., Val Martin, M., Mills, G., Heald, C.L., Harmens, H., Hayes, F., Sharps, K., Bender, J., Ashmore, M.R, 2016. Current and future ozone risks to global terrestrial

biodiversity and ecosystem processes. Ecol. Evol. 6 https://doi.org/10.1002/ece3.2568.
Galmés, J., Flexas, J., Savé, R., Medrano, H., 2007. Water relations and stomatal characteristics of Mediterranean plants with different growth forms and leaf habits: responses to water stress and recovery. Plant Soil 290 (1–2), 139–155.
Gao, Y., Markkanen, T., Thum, T., Aurela, M., Lohila, A., Mammarella, I., Kämäräinen, M., Hagemann, S., Aalto, T., 2016. Assessing various drought indicators in representing summer drought in boreal forests in Finland. Hydrol Earth Syst Sci 20 (1).
García-Gómez, H., Aguillaume, L., Izquieta-Rojano, S., Valiño, F., Àvila, A., Elustondo, D., Santamaría, J.M., Alastuey, A., Calvete-Sogo, H., González-Fernández, I., Alonso, R., 2016a. Atmospheric pollutants in peri-urban forests of Quercus ilex: evidence of pollution abatement and threats for vegetation. Environ. Sci. Pollut. Res. 23, 6400–6413.
García-Gómez, H., Izquieta-Rojano, S., Aguillaume, L., González-Fernández, I., Valiño, F., Elustondo, D., Santamaría, J.M., Àvila, A., Fenn, M.E., Alonso, R, 2016b. Atmospheric deposition of inorganic nitrogen in Spanish forests of Quercus ilex measured with ion-exchange resins and conventional collectors. Environ. Pollut. 216, 653–661.
Genuchten, V.M., 1980. A closed-form equation for predicting the hydraulic conductivity of unsaturated soils. Soil Sci. Soc. Am. J. 44 (5).
Gerosa, G.A., Marzuoli, R., Finco, A., 2022. Interannual variability of ozone fluxes in a broadleaf deciduous forest in Italy. Elementa 10 (1).
Gerosa, G., Marzuoli, R., Monteleone, B., Chiesa, M., Finco, A., 2017. Vertical ozone gradients above forests. comparison of different calculation options with direct ozone measurements above a mature forest and consequences for ozone risk assessment. Forests 8 (9), 337.
González-Fernández, I., Bermejo, V., Elvira, S., Sanz, J., Gimeno, B.S., Alonso, R., 2010. Modelling annual pasture dynamics: application to stomatal ozone deposition. Atmos Environ 44 (21–22).
Grassi, G., Magnani, F., 2005. Stomatal, mesophyll conductance and biochemical limitations to photosynthesis as affected by drought and leaf ontogeny in ash and oak trees. Plant Cell Environ. 28 (7).
Grulke, N.E., Heath, R.L., 2020. Ozone effects on plants in natural ecosystems. Plant Biol. 22 (Issue S1).
Guaita, P.R., Marzuoli, R., Gerosa, G.A., 2023. A regional scale flux-based O3 risk assessment for winter wheat in northern Italy, and effects of different spatio-temporal resolutions. Environ. Pollut. 333.
Guàrdia, R., Arcarons, C.C., Sugrañes, J.M.N., 1998. Phenological patterns in Mediterranean pastures and scrubs of Catalonia/Comportament fenològic de pastures i matollars mediterranis de la Noguera i la plana de Vic. Acta Botánica Barcinonensia (45), 557–576.
Guerreiro, C., Ortiz, A., de Leeuw, F., Viana, M., 2018. Air quality 2018 - EEA report 12 2018.
Hijmans, R.J., 2023. Geographic Data Analysis and Modeling [R Package Raster Version 3.6-26]. https://CRAN.R-project.org/package=raster.
Hunt, E.D., Hubbard, K.G., Wilhite, D.A., Arkebauer, T.J., Dutcher, A.L., 2009. The development and evaluation of a soil moisture index. Int. J. Climatol. 29 (5) https://doi.org/10.1002/joc.1749.
Jakovljević, T., Lovreškov, L., Jelić, G., Anav, A., Popa, I., Fornasier, M.F., Proietti, C., Limić, I., Butorac, L., Vitale, M., de Marco, A., 2021. Impact of ground-level ozone on Mediterranean forest ecosystems health. Sci. Total Environ. 783.
Jarvis, P.G., 1976. The interpretation of the variations in leaf water potential and stomatal conductance found in canopies in the field. Philos. Trans. R. Soc. Lond. B 273 (927).
Juráň, S., Grace, J., Urban, O., 2021. Temporal changes in ozone concentrations and their impact on vegetation. Atmosphere 12 (1).
Kalabokas, P.D., Volz-Thomas, A., Brioude, J., Thouret, V., Cammas, J.P., Repapis, C.C., 2007. Vertical ozone measurements in the troposphere over the Eastern Mediterranean and comparison with Central Europe. Atmos. Chem. Phys. 7 (14).
Karatassiou, M., Noitsakis, B., Koukoura, Z., 2009. Drought adaptation ecophysiological mechanisms of two annual legumes on semi-arid Mediterranean Grassland. Sci. Res. Essays 4 (5), 493–500.
Kask, K., Kaurilind, E., Talts, E., Kännaste, A., Niinemets, Ü., 2021. Combined acute ozone and water stress alters the quantitative relationships between O3 uptake, photosynthetic characteristics and volatile emissions in brassica Nigra. Molecules 26 (11).
Keenan, T., García, R., Friend, A.D., Zaehle, S., Gracia, C., Sabate, S., 2009. Improved understanding of drought controls on seasonal variation in mediterranean forest canopy CO2 and water fluxes through combined *in situ* measurements and ecosystem modelling. Biogeosciences 6 (8).
Klingberg, J., Danielsson, H., Simpson, D., Pleijel, H., 2008. Comparison of modelled and measured ozone concentrations and meteorology for a site in south-west Sweden: implications for ozone uptake calculations. Environ. Pollut. 155 (1).
Kostopoulou, P., Vrahnakis, M.S., Merou, T., Lazaridou, M., 2010. Perennial-like adaptation mechanisms of annual legumes to limited irrigation. J. Environ. Biol. 31 (3), 311–314.
Lemon, J., 2006. Plotrix: A Package in the Red Light District of R. R-News, p. 6.
Levin, A., Nackley, L., 2021. Principles and practices of plant-based irrigation management. Horttechnology 31 (6), 650–660.
Liao, K., Xu, S., Wu, J., Zhu, Q., 2013. Spatial estimation of surface soil texture using remote sensing data. Soil Sci. Plant Nutr. 59 (4).
Limousin, J.M., Rambal, S., Ourcival, J.M., Rocheteau, A., Joffre, R., Rodriguez-Cortina, R., 2009. Long-term transpiration change with rainfall decline in a Mediterranean Quercus ilex forest. Glob. Change Biol. 15 (9).
Lin, M., Horowitz, L.W., Xie, Y., Paulot, F., Malyshev, S., Shevliakova, E., Finco, A., Gerosa, G., Kubistin, D., Pilegaard, K., 2020. Vegetation feedbacks during drought exacerbate ozone air pollution extremes in Europe. Nat. Clim. Change 10 (5).
Martínez-Vilalta, J., Garcia-Forner, N., 2017. Water potential regulation, stomatal behaviour and hydraulic transport under drought: deconstructing the iso/anisohydric concept. Plant Cell Environ. 40 (6).
Martín-Gómez, P., Aguilera, M., Pemán, J., Gil-Pelegrín, E., Ferrio, J.P., 2017. Contrasting ecophysiological strategies related to drought: the case of a mixed stand of Scots pine (Pinus sylvestris) and a submediterranean oak (Quercus subpyrenaica). Tree Physiol. 37 (11).
Marzuoli, R., Bussotti, F., Calatayud, V., Calvo, E., Alonso, R., Bermejo, V., Pollastrini, M., Monga, R., Gerosa, G., 2018. Dose-response relationships for ozone effect on the growth of deciduous broadleaf oaks in mediterranean environment. Atmos. Environ. 190, 331–341.
Mediavilla, S., Escudero, A., 2003. Stomatal responses to drought at a Mediterranean site: a comparative study of co-occurring woody species differing in leaf longevity. Tree Physiol. 23 (14), 987–996.
Mills, G., Hayes, F., Simpson, D., Emberson, L., Norris, D., Harmens, H., Büker, P., 2011. Evidence of widespread effects of ozone on crops and (semi-)natural vegetation in Europe (1990-2006) in relation to AOT40- and flux-based risk maps. Glob. Change Biol. 17 (1).
Mills, G., Pleijel, H., Malley, C.S., Sinha, B., Cooper, O.R., Schultz, M.G., Neufeld, H.S., Simpson, D., Sharps, K., Feng, Z., Gerosa, G., Harmens, H., Kobayashi, K., Saxena, P., Paoletti, E., Sinha, V., Xu, X., 2018. Tropospheric ozone assessment report: present-day tropospheric ozone distribution and trends relevant to vegetation. Elementa 6.
Misson, L., Limousin, J.M., Rodriguez, R., Letts, M.G., 2010. Leaf physiological responses to extreme droughts in Mediterranean Quercus ilex forest. Plant Cell Environ. 33 (11).
Montero, M.J., Obrador, J.J., Cubera, E., Moreno, G., 2004. The role of dehesa land use on tree water status in Central-Western Spain. Adv. Geoecol. 10600 (37).
Moreno, G., Obrador, J.J., Cubera, E., Dupraz, C., 2005. Fine root distribution in Dehesas of Central-Western Spain. Plant Soil 277 (1–2).
Nardini, A., lo Gullo, M.A., Trifilò, P., Salleo, S., 2014. The challenge of the Mediterranean climate to plant hydraulics: responses and adaptations. Environ. Exp. Bot. 103.
Naumann, G., Alfieri, L., Wyser, K., Mentaschi, L., Betts, R.A., Carrao, H., Spinoni, J., Vogt, J., Feyen, L., 2018. Global changes in drought conditions under different levels of warming. Geophys. Res. Lett. 45 (7).
Ochoa-Hueso, R., Munzi, S., Alonso, R., Arróniz-Crespo, M., Avila, A., Bermejo, V., Bobbink, R., Branquinho, C., Concostrina-Zubiri, L., Cruz, C., Cruz de Carvalho, R., de Marco, A., Dias, T., Elustondo, D., Elvira, S., Estébanez, B., Fusaro, L., Gerosa, G., Izquieta-Rojano, S., Theobald, M.R., 2017. Ecological impacts of atmospheric pollution and interactions with climate change in terrestrial ecosystems of the Mediterranean Basin: current research and future directions. Environ. Pollut. 227.
Osakabe, Y., Osakabe, K., Shinozaki, K., Tran, L.S.P., 2014. Response of plants to water stress. Front. Plant Sci. 5 (MAR).
Pardo, F., Gil, L., Pardos, J.A., 1997. Field study of beech (Fagus sylvatica L.) and melojo oak (Quercus pyrenaica willd) leaf litter decomposition in the centre of the Iberian Peninsula. Plant Soil 191 (1).
Pardos, M., Royo, A., Pardos, J.A., 2005. Growth, nutrient, water relations, and gas exchange in a holm oak plantation in response to irrigation and fertilization. New For. 30 (1).
Paterson, S., Minasny, B., McBratney, A., 2018. Spatial variability of Australian soil texture: a multiscale analysis. Geoderma 309.
Pellegrini, E., Hoshika, Y., Dusart, N., Cotrozzi, L., Gérard, J., Nali, C., Vaultier, M.N., Jolivet, Y., Lorenzini, G., Paoletti, E., 2019. Antioxidative responses of three oak species under ozone and water stress conditions. Sci. Total Environ. 647.
Poyatos, R., Llorens, P., Piñol, J., Rubio, C., 2008. Response of Scots pine (Pinus sylvestris L.) and pubescent oak (Quercus pubescens Willd.) to soil and atmospheric water deficits under Mediterranean mountain climate. Ann. For. Sci. 65 (3).
Quero, J.L., Sterck, F.J., Martínez-Vilalta, J., Villar, R., 2011. Water-use strategies of six co-existing Mediterranean woody species during a summer drought. Oecologia 166 (1).
R core team, 2022. R: A language and Environment For Statistical Computing. R Foundation For Statistical Computing. Vienna, Austria. https://www.R-project.org/.
Rambal, S., Ourcival, J.M., Joffre, R., Mouillot, F., Nouvellon, Y., Reichstein, M., Rocheteau, A., 2003. Drought controls over conductance and assimilation of a Mediterranean evergreen ecosystem: scaling from leaf to canopy. Glob. Change Biol. 9 (12).
Rhizopoulou, S., Mitrakos, K., 1990. Water relations of evergreen sclerophylls. I. Seasonal changes in the water relations of eleven species from the same environment. Ann. Bot. 65 (2).
Richter, H., 1997. Water relations of plants in the field: some comments on the measurement of selected parameters. J. Exp. Bot. 48 (306).
Sadras, V.O., Milroy, S.P., 1996. Soil-water thresholds for the responses of leaf expansion and gas exchange: a review. Field Crops Res. 47 (2–3).
Sala, O.E., Lauenroth, W.K., Parton, W.J., 1992. Long-term soil water dynamics in the shortgrass steppe. Ecology 73 (4).
Salleo, S., Gullo, M.A.L., 1990. Sclerophylly and plant water relations in three mediterranean Quercus species. Ann. Bot. 65 (3).
Sanz, J., Calvete-Sogo, H., González-Fernández, I., Lin, J., García-Gómez, H., Muntifering, R., Alonso, R., Bermejo-Bermejo, V., 2015. Foliar senescence is the most sensitive response to ozone in Bromus hordeaceus and is modulated by nitrogen input. Grass Forage Sci. 70 (1).

Schenk, H.J., Jackson, R.B., 2002. Rooting depths, lateral root spreads and below-ground/above-ground allometries of plants in water-limited ecosystems. J. Ecol. 90 (3).
Schmidt, U., Thöni, H., Kaupenjohann, M., 2000. Using a boundary line approach to analyze N2O flux data from agricultural soils. Nutr Cycl Agroecosyst 57 (2).
Schwendenmann, L., Pendall, E., Sanchez-Bragado, R., Kunert, N., Hölscher, D., 2015. Tree water uptake in a tropical plantation varying in tree diversity: interspecific differences, seasonal shifts and complementarity. Ecohydrology 8 (1).
Sellin, A., 1999. Does pre-dawn water potential reflect conditions of equilibrium in plant and soil water status? Acta Oecol. 20, 51–59.
Sicard, P., de Marco, A., Dalstein-Richier, L., Tagliaferro, F., Renou, C., Paoletti, E., 2016. An epidemiological assessment of stomatal ozone flux-based critical levels for visible ozone injury in Southern European forests. Sci. Total Environ. 541.
Simpson, D., Benedictow, A., Berge, H., Bergström, R., Emberson, L.D., Fagerli, H., Flechard, C.R., Hayman, G.D., Gauss, M., Jonson, J.E., Jenkin, M.E., Nyúri, A., Richter, C., Semeena, V.S., Tsyro, S., Tuovinen, J.P., Valdebenito, A., Wind, P., 2012. The EMEP MSC-W chemical transport model; Technical description. Atmos. Chem. Phys. 12 (16).
Simpson, D., Fagerli, H., Jonson, J., et al., 2003. The EMEP Unified Eulerian Model. Model Description.
Simpson, D., González-Fernández, I., Segers, A., Tsyro, S., Valdebento, A., Wind, P., 2022. Updates to the EMEP/MSC-W model, 2021–2022. Transboundary Particulate Matter, Photo-Oxidants, Acidifying and Eutrophying Components. EMEP Status Report 1/2022.
Socias, X., Correia, M.J., Chaves, M., Medrano, H., 1997. The role of abscisic acid and water relations in drought responses of subterranean clover. J. Exp. Bot. 48 (311), 1281–1288.
Szabó, B., Weynants, M., Weber, T.K.D., 2021. Updated European hydraulic pedotransfer functions with communicated uncertainties in the predicted variables (euptfv2). Geosci. Model Dev. 14 (1).
Taylor, K.E., 2001. Summarizing multiple aspects of model performance in a single diagram. J. Geophys. Res. 106 (D7), 7183–7192.
Tognetti, R., Longobucco, A., Miglietta, F., Raschi, A., 1998. Transpiration and stomatal behaviour of Quercus ilex plants during the summer in a Mediterranean carbon dioxide spring. Plant Cell Environ. 21 (6).
Tóth, B., Weynants, M., Pásztor, L., Hengl, T., 2017. 3D soil hydraulic database of Europe at 250 m resolution. Hydrol. Process 31, 2662–2666.
Tuovinen, J.P., Ashmore, M.R., Emberson, L.D., Simpson, D., 2004. Testing and improving the EMEP ozone deposition module. Atmos. Environ. 38 (15).
Val Martin, M., Heald, C.L., Arnold, S.R, 2014. Coupling dry deposition to vegetation phenology in the Community Earth System Model: implications for the simulation of surface O_3. Geophys. Res. Lett. 41 (8).
Verhoef, A., Egea, G., 2014. Modeling plant transpiration under limited soil water: comparison of different plant and soil hydraulic parameterizations and preliminary implications for their use in land surface models. Agric. For. Meteorol. 191.
Viola, F., Daly, E., Vico, G., Cannarozzo, M., Porporato, A., 2008. Transient soil-moisture dynamics and climate change in Mediterranean ecosystems. Water Resour. Res. 44 (11).
Wang, P., Huang, K., Hu, S., 2020. Distinct fine-root responses to precipitation changes in herbaceous and woody plants: a meta-analysis. New Phytol. 225 (4).
Weber, T.K.D., Weynants, M., Szabó, B., 2020. R Package of Updated European Hydraulic Pedotransfer Functions (euptf2). R Package.
Wohlgemuth, H., Mittelstrass, K., Kschieschan, S., Bender, J., Weigel, H.J., Overmyer, K., Kangasjärvi, J., Sandermann, H., Langebartels, C., 2002. Activation of an oxidative burst is a general feature of sensitive plants exposed to the air pollutant ozone. Plant Cell Environ. 25 (6).
Yue, P., Zuo, X., Li, K., Li, X., Wang, S., Ma, X., Qu, H., Chen, M., Liu, L., Misselbrook, T., Yu, Q., 2021. Responses of ecosystem respiration, methane uptake and nitrous oxide emission to drought in a temperate desert steppe. Plant Soil 469 (1–2).
Zanis, P., Hadjinicolaou, P., Pozzer, A., Tyrlis, E., Dafka, S., Mihalopoulos, N., Lelieveld, J., 2014. Summertime free-tropospheric ozone pool over the eastern Mediterranean/middle east. Atmos. Chem. Phys. 14 (1).